Tetramethylpyrazine nitrone exerts neuroprotection via PGC-1α/Nrf2 activation and α-synuclein clearance in Parkinson's disease models

Baojian Guo
Jinan university
Chengyou Zheng
Jinan University College of Pharmacy
Jie Cao
Jinan University College of Pharmacy
Shangming Li
Jinan University College of Pharmacy
Fangcheng Luo
Jinan University College of Pharmacy
Xiaoling Qiu
Jinan University College of Pharmacy
Kun Zhang
Jinan University College of Pharmacy
Wei Cai
Jinan University College of Pharmacy
Haitao Li
University of Macau
Ying Wang
University of Macau
Simon, Mingyuan Lee
University of Macau
Xifei Yang
Shenzhen Center for Disease Control and Prevention
Gaoxiao Zhang
Jinan University College of Pharmacy
Yewei Sun
Jinan University College of Pharmacy
Zaijun Zhang (zaijunzhang@163.com)
Yuqiang Wang
Jinan University College of Pharmacy

Research article

Keywords: Parkinson's disease, tetramethylpyrazine nitrone, peroxisome proliferator-activated receptor γ co-activator 1α, Nuclear factor erythroid-2-related factor 2, α-synuclein

Posted Date: June 10th, 2020

DOI: https://doi.org/10.21203/rs.3.rs-32864/v1

Tetramethylpyrazine nitrone exerts neuroprotection via PGC-1α/Nrf2 activation and α-synuclein clearance in Parkinson's disease models

Baojian Guo[1, 2†], Chengyou Zheng[1,3†], Jie Cao[1†], Shangming Li[1], Fangcheng Luo[1], Xiaoling Qiu[1], Kun Zhang[1], Wei Cai[1], Haitao Li[4], Ying Wang[4], Simon Mingyuan Lee[4], Xifei Yang[5], Gaoxiao Zhang[1]*, Yewei Sun[1]*, Zaijun Zhang[1]* and Yuqiang Wang[1]

[1]Institute of New Drug Research; International Cooperative Laboratory of Traditional Chinese Medicine Modernization and Innovative Drug Development of Chinese Ministry of Education, Jinan University College of Pharmacy, Guangzhou 510632, China.

[2]School of Traditional Chinese Medicine, Jinan University, Guangzhou 510632, China.

[3]School of Chemical Biology and Biotechnology, Shenzhen Graduate School of Peking University, Shenzhen 518055, China.

[4]Institute of Chinese Medical Sciences and State Key Laboratory of Quality Research in Chinese Medicine, University of Macau, Avenida da Universidade, Taipa, Macao SAR, China.

[5]Key Laboratory of Modern Toxicology of Shenzhen, Center for Disease Control and Prevention, No. 8, Longyuan Road, Nanshan District, Shenzhen 518055, China.

†These authors have equal contributions.

*Corresponding author. Email: zhanggaoxiao2005@163.com; yxy0723@163.com; zaijunzhang@163.com.

email addresses:

Baojian Guo, gbj840724918@126.com; Chengyou Zheng, chengyouzheng2017@163.com; Jie Cao, 767142135@qq.com; Shangming Li, 614513805@qq.com; Fangcheng Luo, lfcmike@126.com; Xiaoling Qiu, 13760727828@163.com; Kun Zhang, 1821226734@qq.com; Wei Cai, weicai1991@126.com; Haitao Li, 317778893@qq.com; Ying Wang, emilyywang@um.edu.mo; Simon Mingyuan Lee, SimonLee@um.edu.mo; Xifei Yang, xifeiyang@gmail.com; Gaoxiao Zhang, zhanggaoxiao2005@163.com; Yewei Sun, yxy0723@163.com; Zaijun Zhang, zaijunzhang@163.com; Yuqiang Wang, yqwangphd@gmail.com.

Abstract

Background: The peroxisome proliferator-activated receptor γ co-activator 1α (PGC-1α) and Nuclear factor erythroid 2-related factor 2 (Nrf2) are key regulators controlling antioxidant defense, mitochondrial biogenesis and cellular proteostasis. Dysfunction of these processes has been implicated in the pathogenesis of Parkinson's disease Activation of PGC-1α/Nrf2 might improve mitochondrial dysfunction, promote α-synuclein (α-syn) clearance and attenuate degeneration of nigral dopaminergic neurons in PD.

Methods: Neurotoxin-induced *in vitro* PD model, 1-Methyl-4-phenyl-1, 2, 3, 6-tetrahydropyridine (MPTP)-treated mice model, unilateral intrastriatal injection of 6-hydroxydopamine (6-OHDA)-lesioned rat model, and transgenic mice overexpression of human A53T mutant α-synuclein were used to evaluate the neuroprotective and neurorescue effect of tetramethylpyrazine nitrone (TBN), a free radical scavenger, and its regulation on PGC-1α/Nrf2 pathway.

Results: TBN protected against 1-methyl-4-phenylpyridinium (MPP^+) and 6-OHDA insult in cultured primary midbrain neurons. TBN promoted α-syn clearance by autophagy and proteasomal pathways in cell models overexpressing the human A53T mutant α-syn. In MPTP-treated mice, unilateral 6-OHDA-lesioned rats, and the α-syn transgenic mice model, TBN improved motor impairment, increased survival of nigral dopaminergic neurons, and elevated striatal dopamine levels while decreasing the products of oxidative damage. Importantly, TBN down-regulated the α-syn level in the brain and serum of α-syn-transgenic mice. These *in vitro* and *in vivo* improvements were associated with activation of the PGC-1α/Nrf2 signaling pathway, resulting in reduced oxidative stress, and enhanced mitochondrial functions.

Conclusions: Our work demonstrates that TBN activates PGC-1α/Nrf2 and increases the survival of nigral dopaminergic neurons. These results suggest that TBN warrants further development as a potential new PD treatment.

Keywords: Parkinson's disease; tetramethylpyrazine nitrone; peroxisome proliferator-activated receptor γ co-activator 1α; Nuclear factor erythroid-2-related factor 2; α-synuclein

Background

Parkinson's disease is the second most prevalent long-term neurodegenerative disorder. The disease has both motor and nonmotor manifestations. Motor symptoms are directly associated with degeneration of dopaminergic (DA) neurons in the substantia nigra (SN) [1]. Current therapies for PD include dopamine precursors, dopamine receptor agonists, monoamine oxidase inhibitors, catecholamines, and methyltransferase inhibitors [1]. These dopamine replacement strategies diminish motor deficits in PD patients but lack neuroprotective and/or disease-modifying effects [2]. Although the detailed molecular mechanisms underlying the loss of DA neurons in PD are unclear, increasing evidence suggests that oxidative stress, mitochondrial dysfunction, and abnormal expression and aggregation of α-synuclein (α-syn) each play an important role [1,3]. Several trials targeting individual molecular pathways implicated in PD pathogenesis have failed [4,5]. Therefore, a potentially more powerful strategy is the targeting of co-regulatory molecules that tackle different aspects of PD pathogenesis, such as oxidative stress, mitochondrial dysfunction, and overexpression and aggregation of α-syn in the brain.

Peroxisome proliferator-activated receptor γ co-activator 1α (PGC-1α), a well-known transcriptional co-activator, interacts with nuclear respiratory factors to control the expression of nuclear-encoded mitochondrial proteins that powerfully regulate mitochondrial biogenesis, respiration, and the antioxidant defense system. As a consequence, these proteins exhibit neuroprotective effects through enhancing neuronal activity and reducing neuronal sensitivity to neurotoxins [6-9]. Low expression of the PGC-1α target gene was found in DA neurons of SN in early PD patients [8]. Overexpression of PGC-1α or application of small-molecule PGC-1α activators can improve mitochondrial function and suppress the loss of DA neurons induced by A53T-α-syn and rotenone in rat primary midbrain cultures, as well as protect DA neurons in the MPTP mouse model of PD [8,10].

Abnormal α-syn expression and accumulation of α-syn oligomers disrupt axonal transport, inducing energy deficits that lead to synaptic loss in human neurons [11]. Alpha-syn oligomers can accumulate in and compromise the integrity of the mitochondrial membrane, which impairs the function of mitochondrial complex I and calcium homeostasis, ultimately leading to degeneration and necrosis of DA neurons [12]. On the other hand, under the stimulation of oxidative stress, α-syn accumulates in the nucleus and selectively binds to the promoter of the master mitochondrial transcription co-activator, PGC-1α, then inhibits the transcriptional activity and protein expression of PGC-1α, and further affects the expression of downstream target genes, resulting in structural and functional mitochondrial damage [13]. Nuclear factor erythroid 2-related factor (Nrf2) binds to the antioxidant responsive element (ARE) and exerts an important role in regulating the expression of detoxification genes and oxidative stress-inducible enzymes (e.g., heme oxygenase-1 (HO-1) and NAD(P)H : quinone oxidoreductase-1 (NQO-1)) [14]. More importantly, Nrf2 was recently reported to accelerate the clearance of α-syn by shortening its half-life, leading to lower overall levels of α-syn [15]. Conversely, Nrf2 deficiency and α-syn cooperate in promoting protein aggregation, neuroinflammation and neuronal death in early-stage PD [16]. Indeed, growing evidence also indicates that Nrf2 regulates the expression of autophagy and proteasome subunits involved in protein homeostasis, suggesting that Nrf2 may play an important role in abnormal protein expression and aggregation of misfolded proteins [17]. A direct link between Nrf2 and autophagy was first observed in connection with the adaptor protein p62, also known as SQSTM1, which shuttles ubiquitinated proteins to proteasomal and lysosomal degradation machinery and sequesters damaged proteins into aggregates prior to their degradation [18]. These findings strongly suggest that PGC-1α/Nrf2 might be a co-regulatory molecule in anti-oxidative stress, improvement of mitochondrial dysfunction, and promotion of α-syn clearance. Given this background, we hypothesized that activation of the PGC-1α/Nrf2

signaling pathway could restore the cellular processes that are perturbed in PD and reduce neurodegeneration in cellular and animal models of PD.

Our laboratory has synthesized 2-[[(1,1-dimethylethyl) oxidoimino]-methyl]-3, 5, 6-trimethylpyrazine (tetramethylpyrazine nitrone, TBN). TBN is the result of arming one of the most widely clinically used natural products, 2, 3, 5, 6-tetramethylpyrazine (TMP), with a powerful free-radical scavenging nitrone group [19] (Fig. 1a). The nitrone group is the active pharmacophore of disodium 4-[(*tert*-butylimino)-methyl] benzene-1, 3-disulfonate *N*-oxide (NXY-059, or disufenton sodium, Cerovive), once the subject of intense clinical investigation [20]. TMP is the major component of the medicinal plant *Ligusticum wallichii* Franchat (Chuan Xiong), the use of which was first recorded during the Chinese Tang dynasty. TMP and its derivatives are used for the treatment of ischemic stroke in China. TMP protects neuronal damage in rodent PD models by scavenging free reactive oxidant species [21-25]. NXY-059 exhibits significant neuroprotective activity in neurodegenerative diseases [20,26]; unfortunately, however, NXY-059 failed in Phase III studies for the treatment of ischemic stroke because the drug achieved poor penetration of the blood-brain barrier (BBB) in patients [27]. In sharp contrast to NXY-059, TBN efficiently penetrates BBB and delivers the free-radical scavenging nitrone to the brain to provide neuroprotection [28]. Treatment with TBN attenuates apoptotic cell death of primary hippocampal neurons upon deprivation of oxygen and glucose [29]. TBN exhibits significant protective efficacy in preclinical models of ischemic stroke [28-31], subarachnoid hemorrhage, retinopathy [32] and in rat models of traumatic brain injury [33].

We hypothesized that activating PGC-1α/Nrf2 with TBN would preserve mitochondrial function and promote clearance of abnormal deposits of α-syn. Thus, we tested TBN for its ability to preserve neuronal viability and motor function, as well as its capacity to reduce levels of α-syn and markers of oxidative stress in three animal models of PD, namely MPTP-

and 6-OHDA-induced rodent parkinsonism and hA53T Tg mice. The latter mice overexpress human α-syn and bears the alanine to threonine mutation at residue 53, which causes familial PD.

Two Phase I clinical trials of TBN, by intravenous infusion and oral administration, respectively, have been completed (Trials No. CTR20170564, CTR20180766 and CTR20190583). In these human studies, TBN is safe and well tolerated. TBN is now undergoing two Phase II clinical trials in China for the treatment of ischemic stroke and diabetic kidney disease, respectively.

Methods

Cell culture and treatment

Human neuroblastoma SH-SY5Y and rat pheochromocytoma PC12 cells can synthesize dopamine and norepinephrine and express dopamine transporters. SH-SY5Y cells with stable expression of hA53T mutant α-syn or PC12 cells with Dox-inducible expression of hA53T mutant α-syn were kindly provided by Prof. Yadong Huang (Jinan University, Guangzhou, China) as a gift. Neuro-2a (N2a) cells are a fast-growing mouse neuroblastoma cell line, which has neuronal and amoeboid stem cell morphology. N2a cells were supplied by Prof. Simon MingYuen Lee (State Key Laboratory of Quality Research in Chinese Medicine and Institute of Chinese Medical Sciences, University of Macau, China) as a gift. SH-SY5Y and N2a cells were grown in DMEM supplemented with 10% FBS, 100 U/mL penicillin and 100 μg/mL streptomycin. PC12 cells were cultured in DMEM containing 10% horse serum, 5% FBS, 200 μg/mL G418 in a humidified atmosphere of 5% CO_2 and 95% air at 37 ^{o}C. After treatment, cells were collected and processed for proteasomal activity, dual-luciferase reporter, Western blot and immunofluorescence assays.

Cerebellar granular neurons (CGNs) were isolated from postnatal 8-day old Sprague-Dawley rat pups (15-20 g) according to the protocol described previously [34]. Seven days post-culture, CGNs were processed by TUNEL assay (In situ cell death detection kit, Roche, Mannheim, Germany), MitoCheck mitochondrial complex I activity assay (Cayman Chemical, Ann Arbor, MI. USA) and ATP assay (Beyotime Biotechnology, Nanjing, China).

Primary midbrain neuronal cultures were prepared from the ventral mesencephalon dissected from the embryos of E14 pregnant Sprague-Dawley rats (Animal care facility of SUN YAT-SEN University, Guangzhou, China) as described previously [35]. Five days post-culture,

cells were collected and processed for the 3-(4, 5-Dimethylthiazol-2-yl)-2, 5-Diphenyltetrazolium Bromide (MTT) and Western blot assay, respectively.

Experimental animals

C57BL/6 mice (10-12 weeks old, 25 ± 2 g weight) and SD rats (250 ± 30 g weight) were purchased from Guangdong Medical Laboratory Animal Center (Guangzhou, China). Homozygous transgenic mice of hA53T mutant α-syn (B6; C3-Tg (Prnp-SNA*A53T) 83Vle/JNju) and wild-type littermates were purchased from the Jackson Laboratory (Bar Harbor, ME, USA) and were bred in-house. Animals were housed 3-5 per cage with *ad libitum* access to water and food during a 12 h light/dark cycle.

MPTP mice model

In accordance with our previously published procedure [36], MPTP (30 mg/kg) was administered intraperitoneally (i.p.) once daily for 5 consecutive days to induce experimental Parkinsonism. The control group received an equivalent volume of normal saline. To allow for the full conversion of MPTP to its active neurotoxic metabolite MPP^+, a further 3 days were allowed before drug administration. On day 9, TBN (10, 30 and 90 mg/kg), selegiline (10 mg/kg) or an equal volume of saline was administered intragastrically twice daily for 14 consecutive days.

6-OHDA lesion rat model

Intrastriatal 6-OHDA injection was performed *via* stereotaxic surgery as previously described [37]. Briefly, SD rats were anesthetized with 2.5% isoflurane. A total of 16 μg of 6-OHDA (in 4 μL of 0.9% saline with 0.1% ascorbic acid) was injected into the left striatum at the speed of 1 μL/min through a 10 μL Hamilton® syringe. Detailed coordinates were as following: anterior-posterior: 0 mm, medial-lateral: -1.2 mm, dorsal-ventral: -5.5 and -4.5 mm from bregma. Three weeks after intrastriatal 6-OHDA injection, only rats exhibiting

APO (0.5 mg/kg, i.p.)-induced rotation over 100 turns/30 min were included in the study. Qualifying animals were randomized to different experimental groups. TBN (10, 30 and 60 mg/kg), L-DOPA (25 mg/kg) or an equal volume of saline was administered intragastrically twice daily for 14 consecutive days.

hA53T α-syn transgenic mice model

Ten-month-old hA53T α-syn transgenic mice were treated with TBN (30 mg/kg or 60 mg/kg, i.g. twice daily) or an equal volume of saline for 8 weeks. Age-matched non-transgenic (nTg) littermates given an equal volume of saline were used as the normal controls.

Cellular glycolytic function and oxygen consumption

Cellular glycolytic function and oxygen consumption were monitored according to the manufacturer's protocol (Agilent Cell Analysis Technology, Santa Clara, CA, USA) using the Seahorse XF24 analyzer as previously described [38]. PC12 cells were seeded in Seahorse XF 24-well utility plates (100 μL/well) at a concentration of 2.5×10^5 cells/mL and were cultured for 24 h. The cells were then incubated with the indicated TBN concentration with or without 2 mM MPP^+ for 24 h. The ECAR and OCR parameter values were measured at the indicated time after automatic injection of load compounds in the corresponding well from the appropriate ports of a hydrated sensor cartridge into the identical assay medium. Mitochondrial function parameters were automatically calculated by the Seahorse XF Glycolysis Stress or Mito Stress Test Report Generator.

TUNEL staining

The Click-iT™ plus TUNEL assay (Thermo Fisher Scientific, San Jose CA, USA) was used to detect the apoptotic cells following recommendations from the supplier. Briefly, CGNs were fixed in 4% paraformaldehyde (PFA) for 1 h at room temperature, and were then incubated in permeabilization solution with freshly prepared 0.1% Triton X-100 in 0.1%

sodium citrate for 2 min at 4 ^{o}C. DNA strand breaks were identified by labeling free 3-OH terminals with modified nucleotides in the TUNEL reaction mixture for 1 h at 37 ^{o}C in the dark. The cell nuclei were counterstained with DAPI for 10 min and were viewed with a Laser scanning confocal microscope (Leica TCS SP5, Bensheim, Germany). TUNEL positive cells were calculated from three random fields under 100 X magnification for each treatment group.

Mitochondrial complex I activity

Cellular mitochondria were extracted according to the manufacturer's protocol (Beyotime Biotechnology, Beijing, China). The MitoCheck complex I activity assay (Cayman Chemical, Michigan, USA) was used to test mitochondrial complex I activity. Primary CGNs were pre-treated with TBN (10, 30 and 100 μM) for 2 h followed by 150 μM MPP^{+} treatment for 24 h. Then, CGNs were homogenized with mitochondrial separation reagent on ice for 15 min. The precipitate was removed by centrifugation at 600 g for 10 min at 4 ^{o}C. The supernatant was centrifuged at 11,000 g for 10 min at 4 ^{o}C and then resuspended in isolation buffer. Mitochondrial complex I activity was quantified by measuring the reduction of ubiquinone to ubiquinol following the addition of KCN, NADH and ubiquinone in the presence and absence of rotenone. The absorbance value (OD value) was immediately measured at 340 nm in the plate reader. Mitochondrial complex I activity was expressed as a percentage of the value of the cells without inducer treatment.

ATP determination

ATP levels were determined using a luminescent solution (ATP Determination Kit, Beyotime Biotechnology) according to the manufacturer's protocol. Primary CGNs were pre-treated with TBN (10, 30 and 100 μM) for 2 h followed by 150 μM MPP^{+} treatment for 24 h. Then, CGNs were homogenized with lysis buffer at 12,000 g for 5 min at 4 ^{o}C. The supernatant was

collected and protein concentration was quantitated by BCA assay (Pierce Biotechnology, Rockford, IL, USA). Luminescence values were measured on a microplate reader (BioTek Corporation, Winooski, VT, USA) following the addition of ATP detection reagents. The ATP luminescence (nmol) was determined using a standard curve and was normalized to total protein content (mg) measured by BCA assay.

Luciferase reporter assay of PGC-1α promoter activity

The PGC-1α luciferase reporter assay was carried out as described previously [39]. N2a cells were transiently transfected with 200 ng renilla luciferase-expressing plasmid (pRL-TK, Promega, Madison, WI), 500 ng PGC-1α-2 kb, 500 ng PGC-1α-ΔCRE or 500 ng PGC-1α-ΔMEF plasmid purchased from Addgene (Watertown, Massachusetts, USA) using Lipofectamine® 3000 (Invitrogen, Carlsbad, CA, USA) for 48 h according to the manufacturer's instructions. The pRL-TK plasmid was used as an internal control. Then, cells were pre-treated with 300 μM TBN for 2 h, followed by 2.5 mM MPP^+ treatment for 24 h. Cellular extracts were assessed by the dual-luciferase reporter assay system (Promega, Fitchburg, WI, USA). Luciferase values were normalized to the internal control renilla.

Proteasomal activity assay

The proteasomal chymotrypsin-like, trypsin-like and caspase-like activities were quantified using Proteasome-Glo™ Assay Systems (Promega, Madison, WI, USA) according to manufacturer's instructions. Briefly, PC12 cells were collected and lysed with lysis buffer without SDS. The luminescence was recorded using a microplate reader (BioTek Corporation, Winooski, VT, USA) and normalized to total protein content (mg) measured by BCA assay.

PURE Prep Nuclei assay

Nuclei were isolated from SN tissues or PC12 cells according to the manufacturer's protocol for the PURE Prep Nuclei assay kit (Sigma-Aldrich, St. Louis, MO, USA).

Adenovirus construction

The open reading frame of PGC-1α was amplified using PCR and inserted into the CMV-driven pShuttle-IRES-hrGFP-1 vector from Agilent Technologies. Then, vector was recombined with pAdEasy-1 plasmid to generate the adenovirus-packed expression system. All adenoviruses were amplified in AD-293 cells, purified using CsCl gradient centrifugation, and desalted prior to use.

ELISA measurement

The serum α-syn level was measured using the corresponding Novex® ELISA kit (Life Technologies, Grand Island, NY, USA) according to the manufacturer's instructions. Briefly, all serum samples and standard samples were added to the capture antibody-coated 96-well plate. Then, the biotinylated detection antibody and streptavidin-HRP working solution were added to the plate and incubated at 37 ^{o}C for 1 h. After absorbing the residual liquid in the plate, 50 μL of color developer agent A&B was added to each well and was incubated at 37 ^{o}C for 10 min. Finally, 50 μL of stop solution was added to each well. OD value was measured at 450 nm using a multi-functional microplate reader until the solution turned from blue to yellow. The serum α-syn level was determined by a standard curve generated in the same assay.

Western blotting

SN tissues or cells were homogenized with RIPA lysis buffer containing 1 mM PMSF (Sigma-Aldrich, St. Louis, MO, USA) and 1% halt™ phosphatase inhibitor cocktail (100 X, Thermo Fisher Scientific, MA, USA) on ice. The precipitate was removed by centrifugation at 12,000 g for 30 min at 4 ^{o}C. Total protein concentration of the supernatant was determined using the BCA protein assay kit (Pierce, Rockford, IL). Samples containing 30 μg of protein were separated by 10-15% SDS-PAGE and transferred to PVDF membranes. Then, the

membrane was blocked in 5% (v/v) bovine serum albumin in TBST at room temperature for 2 h. The membranes were incubated with appropriate primary antibodies overnight at 4 ^{o}C, and were then incubated with HRP-conjugated secondary antibody in TBST for 2 h at room temperature (1:2000, Cell Signaling Technology, Danvers, MA, USA). After incubation with secondary antibodies, the reaction product in the membrane was visualized using an ECL advanced Western blotting detection kit (Amersham, Little Chalfont, UK). Western blot images and the densities of the bands were captured and quantitatively assessed using the Care Stream Molecular Imaging Software (Carestream Health Inc, New Haven, CT). Beta-actin, GAPDH, PCNA or Lamin A/C was used as the loading control, respectively. All primary antibodies used in this study are listed in Table S3.

Immunochemistry or Immunofluorescence

Animals in each group were deeply anesthetized with pentobarbital sodium (100 mg/kg, i.p.) and were underwent transcardial perfusion with blood vessel flushing fluid solution (4% PFA in 0.1 M PBS, pH 7.4). The brains were removed and post-fixed for 48 h. The brains were then placed in graded 10% to 30% sucrose solution in 0.1 M PBS, pH 7.4 for 6 days at 4 ^{o}C. Brains were embedded in OCT (Tissue-Tek, Miles Inc., Elkhart, IN), and finally sectioned into 25 μm (MPTP mice model) and 45 μm (6-OHDA rat model) sections. hA53T Tg mice were embedded in paraffin and cut into 5 μm coronal sections encompassing the entire SN. Sections were incubated with 3% hydrogen peroxide (H_2O_2) for 15 min at room temperature to inactivate endogenous peroxidase activity followed by antigen retrieval in sodium citrate buffer (10 mM, pH 6.0) for 15 min at 95 ^{o}C. Cells were immobilized with 4% PFA and brain sections incubated with 0.1% Triton X-100 for 15 min before blocking with 10% horse serum in PBS (0.01 M, pH 7.4) for 2 h at room temperature. Afterward, cells and brain sections were incubated overnight with a primary antibody at 4 ^{o}C. Then, the cells and sections were incubated with appropriate secondary antibodies for 2 h at room temperature. The secondary

antibodies were HRP-linked goat-anti rabbit antibody (1:200, Cell Signaling Technology, Danvers, MA, USA); Alexa Fluor® 546-conjugated goat anti-rabbit or mice (1:200, Invitrogen, Carlsbad, CA, USA) and Alexa Fluor® 488-conjugated goat anti-rabbit or mice (1:200, Invitrogen, Carlsbad, CA, USA). Cell nuclei were counterstained with DAPI for 10 min. Immunohistochemistry (TH-stained sections) was revealed using diaminobenzidine (DAB). Stained cells and tissue slides were viewed with a laser scanning confocal microscope (Leica TCS SP5, Bensheim, Germany). The TH-positive cells in SN were counted with the aid of a stereomicroscope (BX51, Olympus Corp., Tokyo, Japan) using the optical fractionator method as described previously [40]. All primary antibodies used in this study are listed in Table S3.

Total RNA extraction and qRT-PCR

RNA was extracted from the SN with Trizol reagent (Thermo Fisher Scientific, USA). Total RNA (2 μg) was reversely transcribed using M-MuLv Reverse Transcriptase (New England Biolabs, Beverly, MA, USA). Quantitative PCRs were performed in triplicates for all samples using the Mx 3005P Real-Time PCR system (Stratagene) with SYBR Green Supermix (Thermo Fisher Scientific, USA). The reaction condition was the following: 98 ^{o}C for 30 s, then cycling conditions consisting of 40 cycles of 98 ^{o}C, 10 s, 60 ^{o}C, 30 s, 72 ^{o}C, 15 s in 20 μL reaction volumes. Primers used for the qRT-PCR analysis are listed in Table S4 and S5. For normalization, ΔC_t values were calculated relative to the levels of 18S rRNA transcripts. All primers for qRT-PCR were validated prior to use based on the melting curve and C_t value.

TBN tablet pharmacokinetic assessment in healthy Chinese volunteers

The TBN multiple-ascending-dose (MAD) Phase I study in healthy Chinese volunteers has been registered at http://www.chinadrugtrials.org.cn/ (CTR20190583) and conducted in accordance with the Good Clinical Practices and the Declaration of National Medical

Products Administration (NMPA) of China. Twenty-four healthy Chinese volunteers were divided into two groups, one of which received 600 mg of TBN (n=12, male:female=1:1), the other 1200 mg of TBN (n=12, male:female=1:1). Subjects were given the desired amount of TBN in tablet form twice daily (12 h interval) for seven consecutive days. Blood samples were collected in blood collection tubes with EDTA, centrifuged at 1,500 rpm for 10 min, and the supernatant transferred into labeled tubes before freezing at -80 ± 10 ℃ until analysis. TBN's concentrations in serum were measured by HPLC-MS/MS (Waters, Massachusetts, USA).

Statistical and image analysis

Data analyses were performed with GraphPad Prism software 7.0 (GraphPad, San Diego, CA, USA). Results were expressed as Mean ± SEM. An unpaired two-tailed Student's *t* test, one-way or two-way ANOVA and Tukey's multiple comparison tests, were used for comparison between groups. Differences with $P < 0.05$ were considered significant.

Results

TBN protects cultured primary midbrain neurons through PGC-1α activation

We showed previously that TBN protected SH-SY5Y cells from MPP^+-induced cytotoxicity [36]. Here, we tested the neuroprotective effect of TBN on MPP^+- and 6-OHDA-induced neurotoxicity in cultured primary midbrain neurons. Treatment with MPP^+ (20 μM) or 6-OHDA (30 μM) for 24 h resulted in a dramatic decrease in cell viability and in protein expression of tyrosine hydroxylase (TH, a marker of dopaminergic neurons). However, TBN pretreatment (2 h) increased cell viability and TH protein expression level in a concentration-dependent manner, with maximum effect seen at 300 μM (Fig. 1b-e). TBN (300 μM) treatment significantly decreased neuronal apoptosis induced by MPP^+ as determined by TUNEL staining (Fig. S1a).

The neuroprotective effects of TBN were accompanied by increased expression of PGC-1α and its upstream regulators myocyte enhancer-binding factor 2 (MEF2) and sirtuin 1 (SIRT1), all of which contribute to neuronal survival [41] (Fig. 1f, g). By contrast, knockdown of PGC-1α expression by siRNA abolished the neuroprotective effect of TBN (Fig. 1h), demonstrating that PGC-1α is involved in the ability of TBN to protect against neuronal cell death induced by MPP^+. In addition, TBN significantly increased the basal transcriptional activity of PGC-1α, and restored the MPP^+-suppressed transcriptional activity of PGC-1α in N2a cells transfected with a PGC-1α promoter-driven luciferase reporter plasmid. Deletion of the cAMP-response element (CRE) site (PGC-1α-ΔCRE) and a MEF site (PGC-1α-ΔMEF) of the PGC-1α promoter resulted in decreased basal promoter activity and failure to respond to TBN treatment (Fig. 1i), suggesting that the activation of PGC-1α by TBN is CRE- and MEF-dependent.

TBN improves mitochondrial functions

Since PGC-1α is a key co-activator in transcriptional regulation of mitochondrial biogenesis and function [6], we assessed the effects of TBN on mitochondrial function by measuring cellular oxygen consumption rates (OCR) and extracellular acidification rates (ECAR) in PC12 cells incubated with or without TBN plus MPP^+. Under basal conditions, TBN mildly increased the ECAR of maximal glycolysis (Fig. 2a, b). TBN treatment significantly increased the OCR of non-mitochondrial oxygen consumption, spare respiratory capacity (%), coupling efficiency (%), basal respiration, maximal respiratory capacity, and ATP production (Fig. 2c-e). Under the MPP^+-stressed condition, TBN treatment significantly restored the MPP^+-induced decrease in OCR of basal respiration, maximal respiratory capacity, and ATP production (Fig. 2f-i). Accordingly, TBN increased the ATP content and mitochondrial complex I activity in MPP^+-treated primary CGNs in a concentration-dependent manner (Fig. 2j, k). Taken together, TBN enhanced mitochondrial functions, which are crucial for neuronal cell survival.

TBN promotes mutant α-syn clearance through regulation of protein degradation pathways

Aggregation of α-syn is a key hallmark of sporadic and familial PD and contributes to early events of PD pathogenesis, such as oxidative stress and mitochondrial dysfunction [3,42]. To determine the effects of TBN on α-syn protein levels, we used SH-SY5Y cells with stable overexpression of hA53T mutant α-syn, and PC12 cells with doxycycline (Dox)-inducible overexpression of hA53T mutant α-syn. Treatment with MPP^+ or 6-OHDA increased the overexpression of α-syn, but TBN treatment significantly reduced both MPP^+- and 6-OHDA-induced overexpression of α-syn in a concentration-dependent manner (Fig. 3a, b). In

addition, TBN markedly decreased Dox-induced overexpression of α-syn and phosphorylated α-syn (pho-α-syn) (Fig. 3c).

Next, we explored the mechanism underlying the down-regulation of α-syn by TBN, and determined whether activation of the PGC-1α/Nrf2 pathway was involved. To address whether the TBN-mediated decrease of α-syn is due to increased protein degradation, we conducted turnover experiments in the PC12 cells overexpressed mutant α-syn using cycloheximide (CHX), which blocks new protein synthesis. Under these conditions, TBN reduced α-syn levels in the presence of CHX (Fig. S1b), suggesting that α-syn is cleared via modulation of the protein degradation system. Two major systems contribute to proteostasis, namely the ubiquitin proteasome (UPS) and autophagy-lysosomal pathway (ALP). As expected, both MG132 (a proteasome inhibitor) and chloroquine (CQ, a lysosomal inhibitor) completely blocked TBN-induced α-syn clearance (Fig. 3d).

Nrf2 is emerging as a key component of the transduction machinery needed to maintain proteostasis, which is achieved by functions of Nrf2 involved in genes controlling the maintenance of the proteasome and autophagy [17]. PGC-1α and Nrf2 overexpression have previously been shown to reduce α-syn-mediated neurotoxicity in PD models [8,14,15]. In cells with inducible or stable expression of mutant α-syn, under both basal and Dox-/MPP^+-induced conditions, TBN treatment increased the protein expression of PGC-1α, Nrf2 and HO-1, while decreasing the level of α-syn (Fig. 3e, f; Fig S1c-e). TBN also increased the nuclear expression of Nrf2 in Dox-induced PC12 cells (Fig. S1f). In addition, TBN significantly reversed the transcriptional activity of the PGC-1α promoter suppressed by Dox-induced mutant α-syn overexpression (Fig. 3g). Dox induced overexpression of α-syn and simultaneously down-regulated the expression of PGC-1α and Nrf2. However, these

alterations in protein expression were reversed by treatment with both TBN and adenovirus-mediated PGC-1α overexpression, but not by EGFP controlled adenovirus (Fig. 3h). Conversely, specific siRNA-mediated Nrf2 suppression abolished the effect of TBN on Dox-induced α-syn expression in PC12 cells, but scrambled siRNA had no effect (Fig. 3i).

To further confirm that UPS is involved in α-syn clearance by TBN, we measured proteasomal activity and expression of the proteasome subunit. Under basal conditions, TBN treatment significantly increased the trypsin-like, chymotrypsin-like and caspase-like activities (Fig. S2a-c). Under the Dox-stressed condition, TBN treatment dramatically increased chymotrypsin-like, but not trypsin-like and caspase-like activities. MG-132 almost completely inhibited the chymotrypsin-like activity but was ineffective at altering the trypsin-like and caspase-like activities (Fig. S2d-f).

The proteasome subunit beta type-8 (psmb8) is a critical component for the immunoproteasome with its chymotrypsin-like activity in mammals [43]. We found that TBN significantly increased the expression of psmb8 in a concentration-dependent manner (Fig. S2g). In addition, specific siRNA-mediated suppression of Nrf1 or Nrf2 completely abolished the effect of TBN on psmb8 expression, but the scrambled siRNA had no effect (Fig. S2h, i).

Combined with the effect of TBN on proteasomal activity, we propose that TBN promotes A53T-α-syn clearance, as least in part, through increasing proteasomal activity, which is dependent on activation of the PGC-1α/Nrf2 pathway.

TBN's neuroprotective effects in the MPTP-induced mice PD model

To determine whether TBN was neuroprotective in animal models of PD, we firstly examined the effects of TBN on motor behavior and neurodegeneration in the MPTP-induced mice model. The mice were subjected to a sub-acute MPTP regimen, namely, five consecutive daily intraperitoneal injections of MPTP (30 mg/kg/day) [44]. On the third day after the last MPTP injection, TBN (10, 30 and 90 mg/kg) or an equal volume of saline was administered intragastrically twice daily for 14 days (Fig. 4a). MPTP injections resulted in decreased body weight, while TBN treatment slightly increased the body weight of MPTP mice (Fig. 4b). The gait abnormalities of mice in the footprint test were reported to be highly correlated with striatal dopamine content. MPTP injections caused significant impairment of locomotion, with increased time to cross the corridor and decreased stride length. However, TBN at doses of 30 and 90 mg/kg and selegiline, the positive control drug, attenuated these locomotion impairments (Fig. 4c, d).

The brain content of striatal dopamine and its metabolites and the number of TH-positive neurons were examined. As expected, MPTP treatment depleted striatal dopamine and its metabolites 3, 4-dihydroxyphenyl acetic acid (DOPAC) and homovanilic acid (HVA). MPTP treatment also reduced the numbers of TH-positive and normal Nissl-stained neurons, and reduced TH expression in the SN. TBN treatment attenuated these MPTP toxic effects (Fig. 4e-j; Fig S3a, b). Collectively, these results demonstrated that TBN decreased MPTP-induced motor behavioral deficits and neurodegeneration.

TBN's neuroprotective effects in the unilateral 6-OHDA-lesioned rat PD model

The MPTP-induced mice PD model is a bilateral Parkinsonism resulting from systemic MPTP injection. By contrast, injection of 6-OHDA into one side of the striatum creates a unilateral model of Parkinsonism, where the affected and unaffected sides of the brain can be

directly compared. Three weeks after unilateral injection of 6-OHDA (4 μg/μL, 4 μL), rats developed apomorphine (APO)-induced rotation. Rats exhibiting >100 turns/30 min were then administered intragastric TBN twice daily (10, 30 and 60 mg/kg) for 14 days (Fig. 5a). During the experimental period, there was no significant difference in body weight change among the different treatment groups (Fig. 5b). Consistent with previous reports [45], 6-OHDA lesions resulted in locomotion deficits, as shown by reduced performance on the rotarod test (Fig. 5c) and decreased traveled distance in the open-field test (Fig. S3c-f). After 6-OHDA-mediated unilateral striatal lesioning, APO-driven motor activity resulted in contralateral rotations directed toward the side of lesion (Fig. 5d). However, animals treated with TBN exhibited significant and dose-dependent improvements on all behavioral measures, including spontaneous activity in the open-field test, coordination testing in the rotarod test, as well as APO-induced rotation (Fig. 5d and Fig S3c-f). The positive control agent L-DOPA also significantly improved the rotational behavior and locomotion in the open-field test (Fig. 5d and Fig. S3d).

As another measure of protective efficacy of dopaminergic signaling, the striatal dopamine and its metabolites were evaluated. Five weeks after 6-OHDA injection, the ipsilateral striatum, but not the contralateral side, displayed a massive loss of dopamine and its metabolites DOPAC and HVA. TBN treatment significantly increased their levels (Fig. 5e-g). In addition, the time on the rotarod and distance travelled in the open-field showed a significant positive relationship with dopamine content (r^2=0.1573, p=0.0058; and r^2=0.2138, p=0.0009, respectively), while APO-induced rotation showed a significant negative relationship with dopamine content (r^2=0.3299, p< 0.0001) in 6-OHDA rats (Fig. S3g-i).

Consistent with the results of the behavior tests and neurochemical measurements, stereological analyses of immunohistochemically stained brain sections showed that TBN treatment protected the TH-positive SN DA (Fig. 5h, i) and Nissl-stained normal neurons against 6-OHDA neurotoxicity (Fig. S3j, k). Although the positive control agent L-DOPA improved the behavior impairments, it had no obvious neuroprotective effect (Fig. 5h, i). In addition, TBN treatment dose-dependently increased the expression of TH in 6-OHDA rats (Fig. 5j). Taken together, these results demonstrated that TBN could rescue motor behavioral deficits and 6-OHDA-induced neurodegeneration.

TBN's neuroprotective effects in hA53T Tg mice

Aggregated α-syn is a major component of Lewy bodies in PD, and α-syn is genetically linked to both familial and sporadic PD. Since the hA53T Tg mouse model largely reproduces the pathological changes in PD patients [1], we tested whether the neuroprotective effects of TBN could be reproduced in this genetic PD model. Ten-month-old mice were administered TBN (30 mg/kg) via gastric feeding tube twice daily for 8 weeks (Fig. 6a). During the experimental period, there was no significant difference in body weight among the different treatment groups (Fig. 6b). At 10 months of age, the hA53T Tg mice exhibited increased climbing time on the pole test and decreased locomotion in the open-field test compared with nTg animals. In addition, the behavioral deficits of saline-treated hA53T Tg mice progressively increased from 2 weeks before treatment to 8 weeks after treatment (Fig. 6c, d). TBN treatment reduced climbing time on the pole and increased total movement distances in the open-field test. More importantly, TBN slowed or even stopped the progression of behavioral impairments of hA53T Tg mice (Fig. 6c, d). The behavioral deficits of hA53T Tg mice were accompanied by a significant decrease in the number of TH-positive neurons and expression of TH protein in the SN. However, TBN treatment for 8 weeks

markedly attenuated the loss of neurons and increased TH expression (Fig. 6e-g). In the hA53T Tg mice at 10 months of age, 8 weeks of TBN treatment moderately but not significantly reduced the expression of α-syn in the brain SN (Fig. 6g-i). However, TBN treatment significantly reduced serum α-syn levels by 85.6% (Fig. 6j). Collectively, these results showed that TBN had significant therapeutic efficacy in this hA53T Tg mice PD model.

Activation of PGC-1α/Nrf2 signaling pathway in the different *in vivo* PD models

The *in vitro* studies showed that TBN protects midbrain neurons and promotes α-syn clearance *via* regulation of PGC-1α/Nrf2 expression (Fig.1 and Fig. 3). Additional studies sought to determine its mechanism of action in neuroprotection in *in vivo* PD models. From Western blotting analysis of SN samples from MPTP-treated animals, we found that TBN significantly increased the cytosol protein expression of MEF2D, PGC-1α, Nrf2, HO-1 and mitochondrial transcription factor A (TFAM) (Fig. 7a). Bioinformatic analysis and ChIP-qPCR validation identified that PGC-1α was transcriptionally regulated by MEF2; dysfunctional MEF2 might elicit mitochondrial damage and neuronal death [46]. Prior work had also suggested that PGC-1α and MEF2 were functionally linked [41]. MPTP decreased the nuclear protein levels of MEF2D, PGC-1α, Nrf2 and HO-1, while TBN treatment reversed the changes (Fig. 7b). Co-localization of TH and MEF2D or PGC-1α analysis by dual fluorescent immunostaining further verified that TBN increased PGC-1α and MEF2D expression in the DA neurons of MPTP-treated mice (Fig. 7c-f). Biochemical pathways including p38 MAPK, PKA, CDK5 and Akt-GSK-3β all phosphorylate MEF2D directly to control its activity [47]. We found that TBN down-regulated CDK5 and p-GSK-3β expression, and up-regulated p-Akt expression in the brain of MPTP-treated mice (Fig. S4).

Next, in the unilateral 6-OHDA-lesioned rat model, TBN also significantly reversed the down-regulation of PGC-1α induced by 6-OHDA (Fig. 7g). Apart from MEF2D, a large number of signaling molecules, including SIRT1 and cyclin dependent kinase 5 (CDK5), have been proposed to regulate PGC-1α [48]. Accordingly, TBN increased the expression of MEF2D and SIRT1, while decreasing the expression of CDK5 (Fig. 7g). Finally, in the hA53T Tg mice model, co-localization of TH and Nrf2 by dual fluorescent immunostaining revealed that TBN increased Nrf2 expression and its nuclear translocation in the DA neurons (Fig.7h, i). Similarly, the data from Western blotting of SN samples showed that PGC-1α, Nrf2, and HO-1 were all perturbed in the hA53T Tg versus nTg mice. TBN treatment improved all these changes toward the values observed in the nTg mice (Fig. 7j). When mRNA expression in SN samples from MPTP-induced model mice was analyzed, it was found that TBN increased the mRNA expression levels of PGC-1α, MEF2D, Nrf2, HO-1, and TFAM (Fig. S5a-e). Similarly, qRT-PCR analysis of the SN of 6-OHDA unilaterally lesioned rats and hA53T Tg mice showed that TBN increased the mRNA expression of PGC-1α, Nrf1/2 and HO-1 (Fig. S5f-l).

Nrf2 plays a pivotal role in regulating the expression of detoxification genes and oxidative stress-inducible enzymes [49,50]. MPP^+ and 6-OHDA can be sequestered into synaptosomal vesicles, or concentrated within the mitochondria of DA neurons, which leads to reactive oxygen species (ROS) production and results in protein oxidation, lipid peroxidation and DNA oxidative damage. Three-nitrotyrosine (3-NT), 4-hydroxynonenal (4-HNE) and 8-hydroxy-2-deoxyguanosine (8-OHdG) are oxidative products of protein, lipid and DNA, respectively. Immunofluorescence staining showed that 8-OHdG, 4-HNE, and 3-NT levels increased in the SN after MPTP or 6-OHDA treatment. In contrast, TBN treatment significantly reduced the levels of these products (Fig. S6a-h). Aggregation of the α-syn

protein increases oxidative stress [51]; however, TBN remarkably decreased the production of 4-HNE and 3-NT levels in the SN TH-positive neurons of hA53T Tg mice (Fig. S6i-k). Taken together, these results demonstrate that TBN protected the animals from the neurotoxic effects of MPTP and 6-OHDA, as well as α-syn overexpression-induced DA neuron injury and its effects, as measured by the reduced markers of oxidative damage, through activation of the PGC-1α/Nrf2 pathway.

TBN effects on autophagy in PD models

On the basis on our observations *in vitro*, we proposed that TBN reduced α-syn *via* both proteasomal and autophagy pathways (Fig. 3). We already demonstrated that TBN increased proteasomal activity and increased expression of the proteasomal subunit (Fig. S2). We thus focused on autophagy herein. The co-localization analysis between LC3 and Lamp2 revealed that TBN increased autophagolysome formation in TH-positive neurons of both the hA53T Tg and MPTP-induced mice models (Fig. 8a, f). In addition, TBN increased pho-AMPK and reversed expression of different phosphorylated ULK1 in TH-positive neurons (Fig. 8b-e and 8g-j). AMPK, as a master regulator of cellular energy levels, can coordinate cellular energy balance by maintaining intracellular ATP levels within an appropriate range [52]. Consistent with the AMPK-activating effect of TBN, our results showed that TBN increased ATP production and ATP content in MPP^+-induced primary CGNs (Fig. 2i, j). Moreover, AMPK activation inhibits mTOR, and directly phosphorylates the essential protein ULK1 for autophagy initiation to control the autophagy process [53].

Next, we measured the autophagy-related protein and mRNA expression in the MPTP-induced mice model. MPTP decreased the protein expression ratio of pho-AMPK/AMPK. Notably, TBN treatment reversed change in the expression ratio of pho-AMPK/AMPK (Fig.

S7a). In addition, qRT-PCR analysis of mRNA expression in the SN samples showed that TBN elevated the mRNA expression levels of Atg3, Atg5, Atg7, Atg12, Atg13 and ULK1, which were all inhibited by MPTP (Fig. S7b, c). To further examine the effect of TBN on mTOR, we assessed the levels of p70S6K phosphorylation at Thr-389, which was phosphorylated by mTOR. TBN treatment decreased p70S6K phosphorylation, suggesting that TBN may target factors downstream of the p70S6K in PC12 cells with inducible expression of hA53T mutant α-syn (Fig. S7d). We were curious as to whether AMPK, ULK1, and mTOR are direct targets of TBN for regulation autophagy initiation. *An in vitro* kinase assay showed that TBN affected AMPK, ULK1 and mTOR activity (Fig. S7e-g). Collectively, these data suggested that TBN induced autophagy as part of the response that promotes α-syn clearance and prevents neurodegeneration.

Discussion

Disease-modifying therapy that reduces the rate of neurodegeneration or halts disease progress is still one of the greatest unmet needs for PD therapy. TBN is a novel, orally bioavailable, multifunctional neuroprotective agent which is being developed for treatment of PD and other diseases. In the present study, we used both toxin-induced and genetic models of PD to investigate the therapeutic potential of TBN to prevent or slow the progress of neurodegeneration in PD. We found that TBN preserved SN DA neurons and elevated striatal dopamine content in these PD animal models, which translated into an improvement of motor functions accompanied by reduced levels of α-syn and a reduction in markers of oxidative damage. Activation of PGC-1α/Nrf2-related pathways was involved in the mechanism of action of TBN, which provided multiple layers of protection, including improved mitochondrial function, increased anti-oxidative activity, and reduced proteotoxic stress.

In the past few decades, multiple agents attempting disease modification of PD have been tested in clinical trials, but all have failed. An important reason might be the limitations of the currently available animal models of PD. Currently, there is no single animal model of PD that can mimic the full pathology and clinical manifestations of PD [54]. While the MPTP and 6-OHDA rodent models of PD reproduce SN DA neuronal degeneration, the time course and their pathological features differ from those seen in the human disease [1]. Many early attempts at translating preclinical findings to clinical trial outcomes were based only on toxin-induced animal models. Genetic models of PD models (α-syn, pink 1 and other PD-associated proteins) incorporate some additional features of the disease [1]. Combining both genetic and toxin-induced models is likely a better way to test agents for therapeutic potential [4].

In the present study, TBN proved to be consistently effective in both MPTP-induced mice and unilateral 6-OHDA-lesioned rat PD models (Fig. 4, 5), as well as in the hA53T Tg mice

model (Fig. 6). Notably, TBN was administered after the neurodegenerative process had been initiated by MPTP (3 days after the last dose) or 6-OHDA (21 days after 6-OHDA injection) intoxication (Fig. 4a, 5a), in which SN DA neurons continue to die for weeks [55,56]. Similarly, TBN treatment of the hA53T Tg mice started at 10 months of age, when PD-related motor deficits were already developing (Fig. 6a), as shown by animals treated with the vehicle. TBN treatment significantly slowed or even stopped the worsening of motor deficits, apparently modifying the advance of the evolving disease (Fig. 6c, d).

TBN's neuroprotective concentration against both MPTP- and 6-OHDA-induced toxicity in cultured primary midbrain neurons ranged from 30-300 μM. When the rats were administered a single intragastric dose at 45 mg/kg, the plasma concentrations of TBN were 163.09 μM and 119.13 μM, 10 and 30 min after drug administration, respectively. At the same time, the TBN brain concentrations reached approximately 127.70 μM and 100.08 μM, respectively (assuming the volume of 1 g brain tissue is 1 mL) (Table S1). It is clear that TBN's concentration achieves in the brain falls within its neuroprotective concentration range *in vitro*. Most importantly, in the Phase I clinical study, when given to healthy human volunteers at 1200 mg/person orally twice daily for 7 days, the TBN plasma C_{max} reached 114.35 μM (Table S2). These results demonstrate that the TBN therapeutic concentration shown in animal models of PD can be achieved in humans.

Both overproduction of ROS and failure of the anti-oxidative defense system have been reported in PD. Dopamine metabolism promotes oxidative stress [3]. Mitochondrial dysfunction is another source of ROS, which can further damage mitochondria as dopamine oxidation mediates mitochondrial dysfunction in PD [57]. Mitochondrial complex I activity is diminished in the SN of PD patients [58] and the antioxidant protein glutathione is reduced in postmortem PD nigra [59]. Given the role of oxidative stress and mitochondrial dysfunction in PD pathogenesis, agents capable of antioxidation and/or improving mitochondrial function,

725 including coenzyme Q10, creatine and vitamin E, *etc*., have been extensively studied in
726 clinical trials [4]. Although none of these clinical trials have convincingly shown disease-
727 modifying effects, failure of these drugs does not dismiss the major role of mitochondrial
728 dysfunction in PD, and thus should not preclude further investigation into upstream pathways
729 to control mitochondrial function as potential therapeutic targets [60,61]. PGC-1α is a
730 transcriptional co-activator that regulates genes necessary for mitochondrial biogenesis, and it
731 also up-regulates many antioxidant gene activities [6,9]. PGC-1α is suppressed and its level is
732 low early in PD [7,46]. Thus, activation of PGC-1α may be a novel strategy to develop
733 mitochondrial-targeted therapy for early intervention in PD [8,62].

734 Delivery of PGC-1α using an adeno-associated virus (AAV) in specific brain areas shows
735 promising therapeutic value in a model of Alzheimer's disease (AD) [63]. PGC-1α null mice
736 are much more sensitive to the neurodegenerative effects of MPTP, and increasing PGC-1α
737 levels dramatically protects neural cells in culture from oxidative damage or overexpression
738 of A53T α-syn-mediated death [8,9]. However, in the *in vivo* MPTP PD model,
739 overexpression of PGC-1α using AAV results in increased vulnerability to the toxin; this may
740 be due to extraordinarily high levels of PGC-1α suppressing the Pitx3/brain-derived
741 neurotrophic factor (BDNF) pathway [64], which is involved in the development and
742 maintenance of DA neurons [65,66]. Therefore, the precise levels of PGC-1α expression and
743 the method of PGC-1α modulation should be given careful attention to achieve its protective
744 potential while avoiding its potentially deleterious effects [67]. Our present study
745 demonstrated that TBN activated PGC-1α and its downstream events both *in vitro* and *in vivo*
746 (Fig. 1f, g and i; Fig. 3e, f; and Fig. 7), subsequently improving mitochondrial function and
747 reducing markers of oxidative damage, including 8-OHdG, 4-HNE and 3-NT (Fig. S6).
748 Taken together with evidence that silencing PGC-1α (using specific siRNA) significantly
749 abolished the neuroprotective effect of TBN *in vitro* (Fig. 1h), we conclude that PGC-1α is

likely to be a key molecule mediating TBN's neuroprotective effects. Encouragingly, we recently found that TBN increased the protein expression of BDNF in a rat model of ischemic stroke [31], warranting further investigation of the effect TBN has in regulating Pitx3.

Alpha-syn has become an increasingly attractive disease-modifying therapeutic target, as abundant evidence implicates its contributions to PD pathogenesis. Alpha-syn is not only a key contributor to DA neuronal death [12,42] but it also plays a critical role in propagating the neurodegenerative process via a prion-like mechanism [68,69]. PRX002 is a monoclonal antibody designed to preferentially target soluble and insoluble aggregated forms of α-syn. The Phase I study of PRX002 revealed that it was safe and well tolerated; at a dose of 30 mg/kg, it significantly and substantially reduced free serum α-syn levels up to 96.5% within 1 h of the end of the infusion [70,71]. PASADENA, a global Phase II clinical study of PRX002 in early PD patients, is being conducted by Roche (NCT03100149). MEDI1341 is another high-affinity α-syn antibody that can enter the brain, sequester extracellular α-syn and attenuate α-syn spreading *in vivo* [72]. MEDI1341 is now in a Phase I clinical trial sponsored by AstraZeneca, as a novel treatment for PD with the aim of slowing or halting disease progression.

Immunotherapeutic interventions including antibodies against β-amyloid and Tau in AD have been extensively investigated during the last 20 years; however, the results are very disappointing. The constant failures of these immunotherapy trials for AD have raised concerns regarding anti-aggregation targeting across the neurodegenerative disease spectrum [73]. Although α-syn is widely considered to be the primary driver of proteinaceous pathophysiology in PD, dynamic interplay between α-syn and other molecules may not be adequately modulated with anti-α-syn specific immunotherapy. In the present study, we show that the small molecule TBN prompted α-syn clearance both *in vitro* and *in vivo* (Fig. 3; Fig. S1c-e; and Fig. 6g-j). Instead of directly targeting α-syn, TBN up-regulates intrinsic cellular

775 systems. We speculate that TBN is superior to these antibodies because TBN not only lowers
776 the level of α-syn but also protects neurons against oxidative damage and mitochondrial
777 dysfunction in PD.

778 Under normal physiological conditions, α-syn is degraded by both UPS and ALP [74,75].
779 Reduced proteasome activity and expression of UPS subunits have been reported in brains of
780 PD patients [76]. Single-nucleotide polymorphism-based studies have also linked mutations
781 in two UPS enzyme coding genes, parkin and ubiquitin C-terminal hydrolase L1 (UCH-L1),
782 with familial PD [77]. Evidence from human postmortem material, transgenic mice, and
783 cellular models of PD also link α-syn accumulation to alterations in the ALP [78]. A recent
784 study found that elevated mitochondrial oxidant stress in human SN DA neurons triggers
785 dopamine oxidation, leading to lysosomal dysfunction and α-syn accumulation [57]. In our
786 study, both the proteasome inhibitor MG132 and the lysosome inhibitor CQ significantly
787 abolished the α-syn clearance effect of TBN *in vitro* (Fig. 3d), suggesting UPS and ALP are
788 involved in the mechanism underlying TBN's ability to accelerate α-syn degradation. In
789 addition, TBN increased proteasome activity under basal conditions (Fig.S2a-c), especially
790 chymotrypsin-like activity in cells with Dox-induced α-syn overexpression (Fig. S2d-f), and
791 upregulated the protein expression of psmb8 (Fig. S2g, i), a subunit of chymotrypsin-like
792 activity. In hA53T Tg and MPTP-induced mice, TBN increased the co-localization of Lamp2
793 and LC3 (Fig. 8a, f), suggesting that the autophagy system is activated [79]. TBN also
794 increased the expression of proteins and mRNAs involved in autophagic process, including
795 Atg3, Atg5, and ULK1, *etc* (Fig. S7).

796 How does TBN regulate proteasome activity and autophagy? Is activation of the PGC-
797 1α/Nrf2 pathway involved? Growing evidence indicates that Nrf2 regulates the expression of
798 several proteasome subunits and some genes involved in different steps of the autophagic
799 process [17,80,81]. Isabel Lastres-Becker and colleagues have demonstrated that α-syn

overexpression and Nrf2 deficiency cooperate to amplify protein aggregation and promote neuronal death, and targeting Nrf2 with dimethyl fumarate is already in clinical validation as a therapeutic strategy against PD-associated synucleinopathy [16,18]. Our studies showed that TBN consistently up-regulated PGC-1α and Nrf2 expression in all tested cellular and animal models of PD. Specific siRNA targeting of Nrf2 blocked TBN's effects on proteasomal psmb8 stimulation and α-syn clearance (Fig. S2i and Fig. 3i). In contrast, adenovirus-mediated PGC-1α overexpression increased Nrf2 expression and consequently reduced α-syn (Fig. 3h). Together with a recent finding that nuclear α-syn selectively binds to the PGC-1α promoter under conditions of oxidative stress may contribute to losses in mitochondrial function in PD [13]. We summarize a feedback loop regulated by TBN among PGC-1α, Nrf2 and α-syn, which are associated with oxidative stress, mitochondrial dysfunction, and protein degradation pathways UPS and ALP (Fig. 9). However, TBN modulation of autophagy may be more complex than simple Nrf2 activation, as TBN possibly also promoted autophagy by regulating AMPK/ULK1/mTOR signaling (Fig. 8b-e, g-j, and Fig. S7a-d), both of which are intricately tied to autophagy [82].

The limitation of this study is that the exact targets that TBN acts on are not yet clear, although we demonstrate that TBN acts through activation of the PGC-1α/Nrf1/2 pathway and clearance of α-syn in PD models. We cannot rule out the possibility that TBN may also act through other pathways.

Conclusions

Activating PGC-1α/Nrf2 as the therapeutic target is attractive because it affects multiple processes that are implicated in the pathogenesis of PD. These findings should stimulate the development of TBN as a potential disease-modifying therapeutic agent in PD. Given the significant therapeutic efficacy of TBN in different models of PD and its favorable safety and pharmacokinetics profiles in a human Phase I clinical trial, we believe that TBN is a promising new treatment for PD.

Abbreviations

PD: Parkinson's disease; TBN: Tetramethylpyrazine nitrone; DA: dopaminergic; TH: Tyrosine hydroxylase; PGC-1α: peroxisome proliferator-activated receptor γ co-activator 1α; Nrf2: Nuclear factor erythroid-2-related factor 2; α-Syn: α-synuclein

Declarations

Ethical Approval and Consent to participate: All animal studies were conducted according to the guidelines of the Experimental Animal Care and Use Committee of Jinan University, Guangzhou, China. The experimental protocols were approved by the Ethics Committee for Animal Experiments of Jinan University. The TBN multiple-ascending-dose (MAD) Phase I study in healthy Chinese volunteers was approved by the Ethics Committee of Haikou People's Hospital in China. Written informed consent was obtained from each subject.

Consent for publication: Not applicable.

Availability of data and materials: All enquiries regarding TBN should be directed to Y-W S, G-X Z or Z-J Z. TBN will be made available through a material transfer agreement.

Competing interests: Y-W S, G-X Z, Z-J Z and Y-Q W are share owners of Guangzhou Magpie Pharmaceuticals, a company working on the development of TBN as a therapeutic agent for PD therapy. Jinan University holds the patent for TBN. The other authors declare that no competing interests exist.

Funding: This work was partially supported by grants from the National Innovative Drug Program of China (2012ZX09103-101-055 and 2018ZX09301009-001), the National Science Foundation of China (NSFC 81872842), NSFC (31861163001)-Macau Science and Development Fund (FDCT 0004/2018/AFJ) Cooperative Project, Scientific Projects of Guangdong Province (2017A030313742, 2019A020201001 and 2019A1515110751),

873 Scientific Projects of Guangzhou (201704020181 and 201809020008), China Postdoctoral
874 Science Foundation (2018M640886).

875

876 **Author contributions**: Z-J Z, B-J G and C-Y Z designed and performed the experiments and
877 analyzed the data; C-Y Z, J C, K Z and W C participated in experiments with MPTP and 6-
878 OHDA. S-M L and C-Y Z and X-F Y designed and performed the hA53T experiments. F-C L
879 performed the electrochemical HPLC analysis for striatal DA, DOPAC and HVA. X-L Q
880 performed the transfection assay and immunohistochemistry staining studies. S-M Lee and
881 H-T L designed and completed PGC-1α recombinant adenovirus. X-F Y directed the project.
882 Y-W S synthesized TBN. G-X Z, Z-J Z and Y-Q W oversaw the study design and wrote the
883 manuscript. All authors have read and approved the final manuscript.

884

885 **Acknowledgments:** We thank Prof. Spencer Peter for his critical reading and editing of the
886 manuscript. Many thanks also to Linda Wang for editing the manuscript. We also thank Prof.
887 Y. Huang (Jinan University, Guangzhou, China) for providing SH-SY5Y cells with stable
888 expression of hA53T mutant α-syn and PC12 cells with Dox-inducible expression of hA53T
889 mutant α-syn.

890

891

892

893

894

895

References

1. Dauer W, Przedborski S. Parkinson's disease: mechanisms and models. Neuron. 2003;39(6):889-909.
2. Elkouzi A, Vedam-Mai V, Eisinger RS, Okun MS. Emerging therapies in Parkinson disease - repurposed drugs and new approaches. Nat Rev Neurol. 2019;15(4):204-23.
3. Lotharius J, Brundin P. Pathogenesis of Parkinson's disease: dopamine, vesicles and alpha-synuclein. Nat Rev Neurosci. 2002;3(12):932-42.
4. Kalia LV, Kalia SK, Lang AE. Disease-modifying strategies for Parkinson's disease. Mov Disord. 2015;30(11):1442-50.
5. Yacoubian TA, Standaert DG. Targets for neuroprotection in Parkinson's disease. Biochim Biophys Acta. 2009;1792(7):676-87.
6. Wu Z, Puigserver P, Andersson U, Zhang C, Adelmant G, Mootha V, et al. Mechanisms controlling mitochondrial biogenesis and respiration through the thermogenic coactivator PGC-1. Cell. 1999;98(1):115-24.
7. Shin JH, Ko HS, Kang H, Lee Y, Lee YI, Pletinkova O, et al. PARIS (ZNF746) repression of PGC-1alpha contributes to neurodegeneration in Parkinson's disease. Cell. 2011;144(5):689-702.
8. Zheng B, Liao Z, Locascio JJ, Lesniak KA, Roderick SS, Watt ML, et al. PGC-1alpha, a potential therapeutic target for early intervention in Parkinson's disease. Sci Transl Med. 2010;2(52):52ra73.
9. St-Pierre J, Drori S, Uldry M, Silvaggi JM, Rhee J, Jager S, et al. Suppression of reactive oxygen species and neurodegeneration by the PGC-1 transcriptional coactivators. Cell. 2006;127(2):397-408.
10. Mudo G, Makela J, Di Liberto V, Tselykh TV, Olivieri M, Piepponen P, et al. Transgenic expression and activation of PGC-1alpha protect dopaminergic neurons in the MPTP mouse model of Parkinson's disease. Cell Mol Life Sci. 2012;69(7):1153-65.
11. Prots I, Grosch J, Brazdis RM, Simmnacher K, Veber V, Havlicek S, et al. alpha-Synuclein oligomers induce early axonal dysfunction in human iPSC-based models of synucleinopathies. Proc Natl Acad Sci U S A. 2018;115(30):7813-18.

12. Fusco G, Chen SW, Williamson PTF, Cascella R, Perni M, Jarvis JA, et al. Structural basis of membrane disruption and cellular toxicity by alpha-synuclein oligomers. Science. 2017;358(6369):1440-43.
13. Siddiqui A, Chinta SJ, Mallajosyula JK, Rajagopolan S, Hanson I, Rane A, et al. Selective binding of nuclear alpha-synuclein to the PGC1alpha promoter under conditions of oxidative stress may contribute to losses in mitochondrial function: implications for Parkinson's disease. Free Radic Biol Med. 2012;53(4):993-1003.
14. Chen PC, Vargas MR, Pani AK, Smeyne RJ, Johnson DA, Kan YW, et al. Nrf2-mediated neuroprotection in the MPTP mouse model of Parkinson's disease: Critical role for the astrocyte. Proc Natl Acad Sci U S A. 2009;106(8):2933-8.
15. Skibinski G, Hwang V, Ando DM, Daub A, Lee AK, Ravisankar A, et al. Nrf2 mitigates LRRK2- and alpha-synuclein-induced neurodegeneration by modulating proteostasis. Proc Natl Acad Sci U S A. 2017;114(5):1165-70.
16. Lastres-Becker I, Ulusoy A, Innamorato NG, Sahin G, Rabano A, Kirik D, et al. alpha-Synuclein expression and Nrf2 deficiency cooperate to aggravate protein aggregation, neuronal death and inflammation in early-stage Parkinson's disease. Hum Mol Genet. 2012;21(14):3173-92.
17. Pajares M, Cuadrado A, Rojo AI. Modulation of proteostasis by transcription factor NRF2 and impact in neurodegenerative diseases. Redox Biol. 2017;11:543-53.
18. Lastres-Becker I, Garcia-Yague AJ, Scannevin RH, Casarejos MJ, Kugler S, Rabano A, et al. Repurposing the NRF2 Activator Dimethyl Fumarate as Therapy Against Synucleinopathy in Parkinson's Disease. Antioxid Redox Signal. 2016;25(2):61-77.
19. Sun Y, Jiang J, Zhang Z, Yu P, Wang L, Xu C, et al. Antioxidative and thrombolytic TMP nitrone for treatment of ischemic stroke. Bioorg Med Chem. 2008;16(19):8868-74.
20. Lees KR, Zivin JA, Ashwood T, Davalos A, Davis SM, Diener HC, et al. NXY-059 for acute ischemic stroke. N Engl J Med. 2006;354(6):588-600.
21. Bi WF, Yang HY, Liu JC, Cheng TH, Chen CH, Shih CM, et al. Inhibition of cyclic strain-induced endothelin-1 secretion by tetramethylpyrazine. Clin Exp Pharmacol Physiol. 2005;32(7):536-40.

951 22. Lu C, Zhang J, Shi X, Miao S, Bi L, Zhang S, et al. Neuroprotective effects of tetramethylpyrazine
952 against dopaminergic neuron injury in a rat model of Parkinson's disease induced by MPTP. Int J
953 Biol Sci. 2014;10(4):350-7.
954 23. Xu D, Duan H, Zhang Z, Cui W, Wang L, Sun Y, et al. The novel tetramethylpyrazine bis-nitrone
955 (TN-2) protects against MPTP/MPP+-induced neurotoxicity via inhibition of mitochondrial-
956 dependent apoptosis. J Neuroimmune Pharmacol. 2014;9(2):245-58.
957 24. Xu DP, Zhang K, Zhang ZJ, Sun YW, Guo BJ, Wang YQ, et al. A novel tetramethylpyrazine bis-
958 nitrone (TN-2) protects against 6-hydroxyldopamine-induced neurotoxicity via modulation of the
959 NF-kappaB and the PKCalpha/PI3-K/Akt pathways. Neurochem Int. 2014;78:76-85.
960 25. Zhao H, Xu ML, Zhang Q, Guo ZH, Peng Y, Qu ZY, et al. Tetramethylpyrazine alleviated
961 cytokine synthesis and dopamine deficit and improved motor dysfunction in the mice model of
962 Parkinson's disease. Neurol Sci. 2014;35(12):1963-7.
963 26. Maples KR, Green AR, Floyd RA. Nitrone-related therapeutics: potential of NXY-059 for the
964 treatment of acute ischaemic stroke. CNS Drugs. 2004;18(15):1071-84.
965 27. Zivin JA. Clinical trials of neuroprotective therapies. Stroke. 2007;38(2 Suppl):791-3.
966 28. Zhang Z, Zhang G, Sun Y, Szeto SS, Law HC, Quan Q, et al. Tetramethylpyrazine nitrone, a
967 multifunctional neuroprotective agent for ischemic stroke therapy. Sci Rep. 2016;6:37148.
968 29. Zhang G, Zhang T, Wu L, Zhou X, Gu J, Li C, et al. Neuroprotective Effect and Mechanism of
969 Action of Tetramethylpyrazine Nitrone for Ischemic Stroke Therapy. Neuromolecular Med.
970 2018;20(1):97-111.
971 30. Zhang T, Gu J, Wu L, Li N, Sun Y, Yu P, et al. Neuroprotective and axonal outgrowth-promoting
972 effects of tetramethylpyrazine nitrone in chronic cerebral hypoperfusion rats and primary
973 hippocampal neurons exposed to hypoxia. Neuropharmacology. 2017;118:137-47.
974 31. Zhang G, Zhang T, Li N, Wu L, Gu J, Li C, et al. Tetramethylpyrazine nitrone activates the
975 BDNF/Akt/CREB pathway to promote post-ischaemic neuroregeneration and recovery of
976 neurological functions in rats. Br J Pharmacol. 2018;175(3):517-31.
977 32. Luo X, Yu Y, Xiang Z, Wu H, Ramakrishna S, Wang Y, et al. Tetramethylpyrazine nitrone
978 protects retinal ganglion cells against N-methyl-d-aspartate-induced excitotoxicity. J Neurochem.
979 2017;141(3):373-86.

33. Zhang G, Zhang F, Zhang T, Gu J, Li C, Sun Y, et al. Tetramethylpyrazine Nitrone Improves Neurobehavioral Functions and Confers Neuroprotection on Rats with Traumatic Brain Injury. Neurochem Res. 2016;41(11):2948-57.
34. Zhou X, Zhu L, Wang L, Guo B, Zhang G, Sun Y, et al. Protective Effect of Edaravone in Primary Cerebellar Granule Neurons against Iodoacetic Acid-Induced Cell Injury. Oxidative medicine and cellular longevity. 2015;2015:606981.
35. Frank LE, Caldera-Siu AD, Pothos EN. Primary dissociated midbrain dopamine cell cultures from rodent neonates. Journal of visualized experiments : JoVE. 2008(21).
36. Guo B, Xu D, Duan H, Du J, Zhang Z, Lee SM, et al. Therapeutic effects of multifunctional tetramethylpyrazine nitrone on models of Parkinson's disease in vitro and in vivo. Biol Pharm Bull. 2014;37(2):274-85.
37. Wang Z, Myers KG, Guo Y, Ocampo MA, Pang RD, Jakowec MW, et al. Functional reorganization of motor and limbic circuits after exercise training in a rat model of bilateral parkinsonism. PLoS One. 2013;8(11):e80058.
38. Zhang J, Nuebel E, Wisidagama DR, Setoguchi K, Hong JS, Van Horn CM, et al. Measuring energy metabolism in cultured cells, including human pluripotent stem cells and differentiated cells. Nat Protoc. 2012;7(6):1068-85.
39. Cheng A, Wan R, Yang JL, Kamimura N, Son TG, Ouyang X, et al. Involvement of PGC-1α in the formation and maintenance of neuronal dendritic spines. 2012;3(3):1250.
40. Finkelstein DI, Stanic D, Parish CL, Drago J, Horne MK. Quantified assessment of terminal density and innervation. Curr Protoc Neurosci. 2004;Chapter 1:Unit 1 13.
41. Handschin C, Spiegelman BM. Peroxisome proliferator-activated receptor gamma coactivator 1 coactivators, energy homeostasis, and metabolism. Endocr Rev. 2006;27(7):728-35.
42. Mor DE, Tsika E, Mazzulli JR, Gould NS, Kim H, Daniels MJ, et al. Dopamine induces soluble alpha-synuclein oligomers and nigrostriatal degeneration. Nat Neurosci. 2017;20(11):1560-68.
43. Akiyama K, Yokota K, Kagawa S, Shimbara N, Tamura T, Akioka H, et al. cDNA cloning and interferon gamma down-regulation of proteasomal subunits X and Y. Science. 1994;265(5176):1231-4.

44. Jackson-Lewis V, Przedborski S. Protocol for the MPTP mouse model of Parkinson's disease. Nat Protoc. 2007;2(1):141-51.

45. Ferro MM, Bellissimo MI, Anselmo-Franci JA, Angellucci MEM, Canteras NS, Da Cunha C. Comparison of bilaterally 6-OHDA- and MPTP-lesioned rats as models of the early phase of Parkinson's disease: Histological, neurochemical, motor and memory alterations. Journal of Neuroscience Methods. 2005;148(1):78-87.

46. Ryan SD, Dolatabadi N, Chan SF, Zhang X, Akhtar MW, Parker J, et al. Isogenic human iPSC Parkinson's model shows nitrosative stress-induced dysfunction in MEF2-PGC1alpha transcription. Cell. 2013;155(6):1351-64.

47. Yin Y, She H, Li W, Yang Q, Guo S, Mao Z. Modulation of Neuronal Survival Factor MEF2 by Kinases in Parkinson's Disease. Front Physiol. 2012;3:171.

48. Ventura-Clapier R, Garnier A, Veksler V. Transcriptional Control of Mitochondrial Biogenesis: the Central Role of PGC-1 alpha. Cardiovascular Research. 2008;79(2):208-17.

49. Pei-Chun C, Vargas MR, Pani AK, Smeyne RJ, Johnson DA, Yuet Wai K, et al. Nrf2-mediated neuroprotection in the MPTP mouse model of Parkinson's disease: Critical role for the astrocyte. Proceedings of the National Academy of Sciences of the United States of America. 2009;106(8):2933-38.

50. Yoo MS, Chun HS, Son JJ, DeGiorgio LA, Kim DJ, Peng C, et al. Oxidative stress regulated genes in nigral dopaminergic neuronal cells: correlation with the known pathology in Parkinson's disease. Molecular Brain Research. 2003;110(1):76-84.

51. Giasson BI, Duda JE, Murray IV, Chen Q, Souza JM, Hurtig HI, et al. Oxidative damage linked to neurodegeneration by selective alpha-synuclein nitration in synucleinopathy lesions. Science. 2000;290(5493):985-9.

52. Cordero MD, Viollet B. AMP-activated Protein Kinase. Xpharm the Comprehensive Pharmacology Reference. 2008;246(4):32-32.

53. Pui-Mun W, Cindy P, Ganley IG, Xuejun J. The ULK1 complex: sensing nutrient signals for autophagy activation. Autophagy. 2013;9(2):124-37.

54. Beal MF. Parkinson's disease: a model dilemma. Nature. 2010;466(7310):S8-10.

55. Jackson-Lewis V, Jakowec M, Burke RE, Przedborski S. Time course and morphology of dopaminergic neuronal death caused by the neurotoxin 1-methyl-4-phenyl-1,2,3,6-tetrahydropyridine. Neurodegeneration. 1995;4(3):257-69.

56. Jeon BS, Jackson-Lewis V, Burke RE. 6-Hydroxydopamine lesion of the rat substantia nigra: time course and morphology of cell death. Neurodegeneration. 1995;4(2):131-7.

57. Burbulla LF, Song P, Mazzulli JR, Zampese E, Wong YC, Jeon S, et al. Dopamine oxidation mediates mitochondrial and lysosomal dysfunction in Parkinson's disease. Science. 2017;357(6357):1255-61.

58. Gatt AP, Duncan OF, Attems J, Francis PT, Ballard CG, Bateman JM. Dementia in Parkinson's disease is associated with enhanced mitochondrial complex I deficiency. Mov Disord. 2016;31(3):352-9.

59. Sofic E, Lange KW, Jellinger K, Riederer P. Reduced and oxidized glutathione in the substantia nigra of patients with Parkinson's disease. Neurosci Lett. 1992;142(2):128-30.

60. Abeliovich A. Parkinson's disease: Mitochondrial damage control. Nature. 2010;463(7282):744-5.

61. Bingol B, Tea JS, Phu L, Reichelt M, Bakalarski CE, Song Q, et al. The mitochondrial deubiquitinase USP30 opposes parkin-mediated mitophagy. Nature. 2014;510(7505):370-5.

62. Schapira AH, Olanow CW, Greenamyre JT, Bezard E. Slowing of neurodegeneration in Parkinson's disease and Huntington's disease: future therapeutic perspectives. Lancet. 2014;384(9942):545-55.

63. Katsouri L, Lim YM, Blondrath K, Eleftheriadou I, Lombardero L, Birch AM, et al. PPARgamma-coactivator-1alpha gene transfer reduces neuronal loss and amyloid-beta generation by reducing beta-secretase in an Alzheimer's disease model. Proc Natl Acad Sci U S A. 2016;113(43):12292-97.

64. Clark J, Silvaggi JM, Kiselak T, Zheng K, Clore EL, Dai Y, et al. Pgc-1alpha overexpression downregulates Pitx3 and increases susceptibility to MPTP toxicity associated with decreased Bdnf. PLoS One. 2012;7(11):e48925.

65. Maxwell SL, Ho HY, Kuehner E, Zhao S, Li M. Pitx3 regulates tyrosine hydroxylase expression in the substantia nigra and identifies a subgroup of mesencephalic dopaminergic progenitor neurons during mouse development. Dev Biol. 2005;282(2):467-79.

66. van den Munckhof P, Luk KC, Ste-Marie L, Montgomery J, Blanchet PJ, Sadikot AF, et al. Pitx3 is required for motor activity and for survival of a subset of midbrain dopaminergic neurons. Development. 2003;130(11):2535-42.
67. Lindholm D, Eriksson O, Makela J, Belluardo N, Korhonen L. PGC-1alpha: a master gene that is hard to master. Cell Mol Life Sci. 2012;69(15):2465-8.
68. Cavaliere F, Cerf L, Dehay B, Ramos-Gonzalez P, De Giorgi F, Bourdenx M, et al. In vitro alpha-synuclein neurotoxicity and spreading among neurons and astrocytes using Lewy body extracts from Parkinson disease brains. Neurobiol Dis. 2017;103:101-12.
69. Olanow CW, Brundin P. Parkinson's disease and alpha synuclein: is Parkinson's disease a prion-like disorder? Mov Disord. 2013;28(1):31-40.
70. Jankovic J, Goodman I, Safirstein B, Marmon TK, Schenk DB, Koller M, et al. Safety and Tolerability of Multiple Ascending Doses of PRX002/RG7935, an Anti-alpha-Synuclein Monoclonal Antibody, in Patients With Parkinson Disease: A Randomized Clinical Trial. JAMA Neurol. 2018;75(10):1206-14.
71. Schenk DB, Koller M, Ness DK, Griffith SG, Grundman M, Zago W, et al. First-in-human assessment of PRX002, an anti-alpha-synuclein monoclonal antibody, in healthy volunteers. Mov Disord. 2017;32(2):211-18.
72. Schofield DJ, Irving L, Calo L, Bogstedt A, Rees G, Nuccitelli A, et al. Preclinical development of a high affinity alpha-synuclein antibody, MEDI1341, that can enter the brain, sequester extracellular alpha-synuclein and attenuate alpha-synuclein spreading in vivo. Neurobiol Dis. 2019;132:104582.
73. Selkoe DJ. Alzheimer disease and aducanumab: adjusting our approach. Nat Rev Neurol. 2019;15(7):365-66.
74. Paxinou E, Chen Q, Weisse M, Giasson BI, Norris EH, Rueter SM, et al. Induction of alpha-synuclein aggregation by intracellular nitrative insult. J Neurosci. 2001;21(20):8053-61.
75. Webb JL, Ravikumar B, Atkins J, Skepper JN, Rubinsztein DC. Alpha-Synuclein is degraded by both autophagy and the proteasome. J Biol Chem. 2003;278(27):25009-13.
76. McNaught KS, Jenner P. Proteasomal function is impaired in substantia nigra in Parkinson's disease. Neurosci Lett. 2001;297(3):191-4.

77. Dawson TM, Dawson VL. Rare genetic mutations shed light on the pathogenesis of Parkinson disease. J Clin Invest. 2003;111(2):145-51.

78. Xilouri M, Brekk OR, Stefanis L. Autophagy and Alpha-Synuclein: Relevance to Parkinson's Disease and Related Synucleopathies. Mov Disord. 2016;31(2):178-92.

79. Kirkegaard K, Jackson WT. Topology of double-membraned vesicles and the opportunity for non-lytic release of cytoplasm. Autophagy. 2005;1(3):182-4.

80. Ugun-Klusek A, Tatham MH, Elkharaz J, Constantin-Teodosiu D, Lawler K, Mohamed H, et al. Continued 26S proteasome dysfunction in mouse brain cortical neurons impairs autophagy and the Keap1-Nrf2 oxidative defence pathway. Cell Death Dis. 2017;8(1):e2531.

81. Tsvetkov AS, Arrasate M, Barmada S, Ando DM, Sharma P, Shaby BA, et al. Proteostasis of polyglutamine varies among neurons and predicts neurodegeneration. Nat Chem Biol. 2013;9(9):586-92.

82. Klionsky DJ, Emr SD. Autophagy as a regulated pathway of cellular degradation. Science. 2000;290(5497):1717-21.

Figure legends

Fig. 1 TBN protects primary midbrain neurons against MPP^+ and 6-OHDA-induced toxicity through activation of PGC-1α. **a** Chemical structure of TMP, NXY-059 and TBN. Primary midbrain neurons were pre-treated with indicated concentrations of TBN for 2 h followed by treatment with 20 μM MPP^+ or 30 μM 6-OHDA for 24 h **(b-g)**. **b, d** Effect on cell viability of MPP^+- or 6-OHDA-treated neurons. **c, e** Western blot for TH expression in MPP^+- or 6-OHDA-treated neurons. **f, g** Western blot for expression of MEF2D, SIRT1 or PGC-1α in MPP^+- or 6-OHDA-treated neurons. **h** Silencing of PGC-1α by specific siRNA abolished the protective effect of TBN in MPP^+-treated neurons. **i** TBN increased MEF- and CRE-dependent PGC-1α promoter transcriptional activity. Data are expressed as means ± SEM of three independent experiments. $^{*}P < 0.05$, $^{**}P < 0.01$ and $^{***}P < 0.001$ versus untreated control group. $^{\#}P < 0.05$, $^{\#\#}P < 0.01$ and $^{\#\#\#}P < 0.001$ versus MPP^+ or 6-OHDA alone group. $^{\$\$\$}P < 0.001$ and $^{\&\&\&}P < 0.001$. Data were analyzed using one-way ANOVA and Tukey's multiple comparison tests.

Fig. 2 TBN increases PC12 cells mitochondrial functions. **a**, **b** ECAR response curve and maximal glycolysis. **c**-**e** OCR response curve and non-mitochondrial oxygen consumption, spared respiratory capacity (%), coupling efficiency (%), basal respiration, maximal respiration and ATP production. **f** Response curve of OCR after TBN treatment of MPP^+-induced PC12 cells. **g** Basal respiration. **h** maximal respiration. **i** ATP production. **j** ATP content and (**k**) Mitochondrial complex I activity in CGNs. Data are means ± SEM of three independent experiments. $^{*}P < 0.05$, $^{**}P < 0.01$ and $^{***}P < 0.001$ versus untreated control group. $^{\#}P < 0.05$, $^{\#\#}P < 0.01$ and $^{\#\#\#}P < 0.001$ versus MPP^+ alone group. Data were analyzed using unpaired Student's *t* test (**b**, **d**, **e**) or one-way ANOVA and Tukey's multiple comparison test (**g**-**k**).

Fig. 3 TBN promotes α-syn clearance through activation of PGC-1α/Nrf2. **a**, **b** Effect of TBN on the level of α-syn protein in SH-SY5Y cells with stable expression hA53T mutant α-syn, which were pre-treated with TBN at indicated concentrations for 2 h followed by 2 mM MPP^+ (**a**) or 200 μM 6-OHDA (**b**) treatment for 24 h. **c** Effect of TBN on the protein levels of α-syn and pho-α-syn in PC12 cells with Dox-inducible expression of hA53T mutant α-syn, which were incubated with 1 μg/mL Dox in the presence or absence of TBN for another 24 h. **d** Both the proteasomal inhibitor MG132 and the lysosomal inhibitor CQ abolished the effect of TBN. Cells were pre-treated with 20 μM CQ or 0.7 μM MG132 for 2 h followed by treatment as in (**c**). **e**, **f** TBN concentration-dependently increased protein expression of PGC-1α, Nrf2 and HO-1 at basal (**e**) and Dox-stressed conditions (**f**) in PC12 cells with inducible expression of hA53T mutant α-syn. **g** TBN increased transcriptional activity of the PGC-1α promoter in Dox-induced PC12 cells. **h** Adenovirus-guided PGC-1α overexpression increased Nrf2 expression, but decreased α-syn levels in Dox-induced PC12 cells. **i** Down-regulation of Nrf2 by specific siRNA abolished the effect of TBN on α-syn clearance in Dox-induced PC12 cells. Data are means ± SEM of three independent experiments $^{*}P < 0.05$, $^{**}P < 0.01$ and $^{***}P < 0.001$ versus untreated control group. $^{\#}P < 0.05$, $^{\#\#}P < 0.01$ and $^{\#\#\#}P < 0.001$ versus MPP^+ or 6-OHDA or Dox alone group. Data were analyzed using one-way ANOVA (**a**-**i**) and Tukey's multiple comparison tests.

Fig. 4 TBN improves motor behavior and protects SN neurons in the MPTP-induced mice PD model. **a** Experimental schedule. **b** Body weight. **c** Time taken to cross the corridor (s). **d** Stride length (cm) in the footprint test. **e-g** Quantification of striatal DA, DOPAC and HVA by HPLC. **h** Representative photomicrographs of immunohistochemistry staining for TH in the SN of MPTP mice. Scale bars, 100 μm. **i** Stereological counting of TH-positive neurons from SN. **j** Western blot for TH expression in the SN of MPTP mice. Data are means ± SEM

of 15-16 mice per group in motor behavior test, and of 6-8 mice per group in biochemical, pathological and Western blot analyzes. $^{*}P < 0.05$ and $^{**}P < 0.01$ versus sham group; $^{\#}P < 0.05$, $^{\#\#}P < 0.01$ and $^{\#\#\#}P < 0.001$ versus MPTP alone group. Data were analyzed using one-way ANOVA and Tukey's multiple comparison tests.

Fig. 5 TBN improves motor behavior and protects SN neurons in the 6-OHDA-induced rat PD model. **a** Experimental schedule. **b** Body weight. **c** Time on the rotarod (s). **d** Contralateral rotations in 30 min after APO injection. **e**-**g** Quantification of striatal DA, DOPAC and HVA by HPLC. **h** Representative photomicrographs of immunohistochemistry staining for TH in SN. Scale bars, 200 μm. **i** Stereological counting of TH-positive neurons from SN. **j** Western blot for TH expression in SN of 6-OHDA rats. Data were means ± SEM of 9-13 rats per group in motor behavior test, and of 5-7 rats per group in biochemical, pathological and Western blot analyses. $^{**}P < 0.01$ and $^{***}P < 0.001$ versus sham group; $^{\#}P < 0.05$ and $^{\#\#}P < 0.01$ versus 6-OHDA alone group. Data were analyzed using two-way (**b**-**d**) or one-way ANOVA (**e**-**j**) and Tukey's multiple comparison tests.

Fig. 6 TBN improves motor behavior and protects SN neurons in the hA53T α-syn transgenic mice PD model. **a** Experimental schedule. **b** Body weight. **c** Climbing time on pole test (% of nTg). **d** Total distance travelled (% of nTg). **e** Representative photomicrographs of immunofluorescence staining for TH in SN. Scale bars, 100 μm, but 50 μm for zoon in. **f** Stereological counting of TH-positive neurons from SN. **g** Western blot for TH and α-syn expression in SN of hA53T α-syn transgenic mice. **h** Representative photomicrographs of immunofluorescence staining for α-syn in brain sections. Scale bars, 50 μm, but 10 μm when zoomed in. **i** Intensity of α-syn in the SN [a.u. (arbitrary units)]. **j** Quantification of α-syn

contents in the serum by ELISA. Data are means ± SEM of 7-9 mice per group for all measurements. $^{**}P < 0.01$ and $^{***}P < 0.001$ versus nTg group; $^{\#}P < 0.05$, $^{\#\#}P < 0.01$ and $^{\#\#\#}P < 0.001$ versus hA53T α-syn Tg mice model group. Data were analyzed using two-way (**b**-**d**) or one-way ANOVA (**f**, **g**, **i** and **j**) and Tukey's multiple comparison tests.

Fig. 7 TBN activates PGC-1α/Nrf2 pathway in the animal PD models. **a** Western blot for expression of MEF2D, PGC-1α, Nrf2, HO-1 and TFAM in the cytosol of SN tissue from MPTP mice. **b** Western blot for expression of MEF2D, PGC-1α, Nrf2, and HO-1 in the nuclei of SN tissue from MPTP mice. **c**, **d** Representative photomicrographs of co-immunofluorescence staining for TH (red), MEF2D (green), and DAPI (blue) (**c**), and for TH (green), PGC-1α (red), and DAPI (blue) (**d**) in the SN of MPTP mice. Scale bars, 20 μm. **e**, **f** Intensity of MEF2D and PGC-1α in the TH-positive neurons. **g** Western blot for expression of SIRT1, MEF2D, CDK5 and PGC-1α in the SN of 6-OHDA rats. **h** Representative photomicrographs of co-immunofluorescence for TH (green), Nrf2 (red), and DAPI (blue) in the SN of hA53T Tg mice. Scale bars, 25 μm. Boxed areas are shown at a higher magnification in the right panel. Arrows indicate co-localization of TH and Nrf2, and nuclear translocation of Nrf2. **i** Fluorescence intensity ratio of Nrf2 in the TH-positive neurons. **j** Western blot for expression of PGC-1α, HO-1, and Nrf2 in the SN of hA53T Tg mice. Data were means ± SEM of 6 animals per group. $^{*}P < 0.05$, $^{**}P < 0.01$ and $^{***}P < 0.001$ versus sham or nTg group; $^{\#}P < 0.05$, $^{\#\#}P < 0.01$ and $^{\#\#\#}P < 0.001$ versus model group. Data were analyzed using one-way ANOVA and Tukey's multiple comparison tests.

Fig. 8 TBN activates autophagy in hA53T α-syn Tg and MPTP-induced mice PD model. **a**-**c** Representative photomicrographs of co-immunofluorescence staining for Lamp2 (green),

LC3 (red), TH (purple) and DAPI (light blue) (**a**), for TH (green), pho-AMPK (Thr 172) (red) and DAPI (blue) (**b**), and for TH (green), pho-ULK1 (Ser 757) (red) and DAPI (blue) (**c**) in the SN of hA53T α-syn Tg mice. Scale bars, 20 μm, but 10 μm when zoomed in. **d**, **e** Intensity of pho-AMPK (Thr 172) and pho-ULK1 (Ser 757) in the TH-positive neurons [a.u. (arbitrary units)]. **f**-**h** Representative photomicrographs of co-immunofluorescence staining for Lamp2 (green), LC3 (red), TH (purple) and DAPI (light blue) (**f**), for TH (green), pho-AMPK (Thr 172) (red) and DAPI (blue) (**g**), and for TH (green), pho-ULK1 (Ser 555) (red) and DAPI (blue) (**h**) in the SN of MPTP mice. Scale bars, 20 μm, but 10 μm when zoomed in. **i**, **j** Intensity of pho-AMPK (Thr 172) and pho-ULK1 (Ser 555) in the TH-positive neurons [a.u. (arbitrary units)]. Boxed areas in **a** and **f** are shown at a higher magnification in the right panel. Arrows indicate co-localization of Lamp2, LC3 and TH. The co-localization between LC3 and Lamp2 are illustrated by line profile. $^{***}P < 0.001$ versus sham or nTg group; $^{\#\#}P < 0.01$ versus model group. Data were analyzed using one-way ANOVA and Tukey's multiple comparison tests.

Fig. 9. Schematic diagram of proposed TBN's mechanisms of action in experimental PD models. TBN suppresses oxidative stress to activate the AMPK/PGC-1α/Nrf1/2 signaling pathway, resulting in reduced oxidative stress, enhanced mitochondrial function and increased protein clearance, eventually preventing the advance of nigral dopaminergic neurodegeneration in experimental models of PD.

Additional file 1

Fig. S1. TBN protects CGNs from MPP^+-induced apoptosis and decreases α-syn through activation of PGC-1α and Nrf2 in cells overexpressing α-syn.

Fig. S2. TBN increases proteasomal enzyme activity under basal and Dox-stressed conditions in PC12 cells.

Fig. S3. TBN improves motor dysfunction and prevents neurodegeneration in MPTP-/6-OHDA-induced PD models.

Fig. S4. TBN regulates AKT/GSK3β and CDK5 protein expression in MPTP-induced mice PD model.

Fig. S5. TBN increases mRNA expression of genes related to PGC-1α/Nrf2 pathway in the SN of PD models.

Fig. S6. TBN decreases products of oxidative damage in SN of animal PD models.

Fig. S7. TBN regulates the expression of autophagy-related proteins and genes in MPTP-induced mice PD model.

Table S1. TBN concentration in the plasma and brain of rats after a single 45 mg/kg intragastric administration.

Table S2. TBN pharmacokinetics in healthy Chinese volunteers after multiple-dose administration for 7 days.

Table S3. Information about primary antibodies used.

Table S4. Mouse primer sequence used for qRT-PCR.

Table S5. Rat primer sequence used for qRT-PCR.

Figures

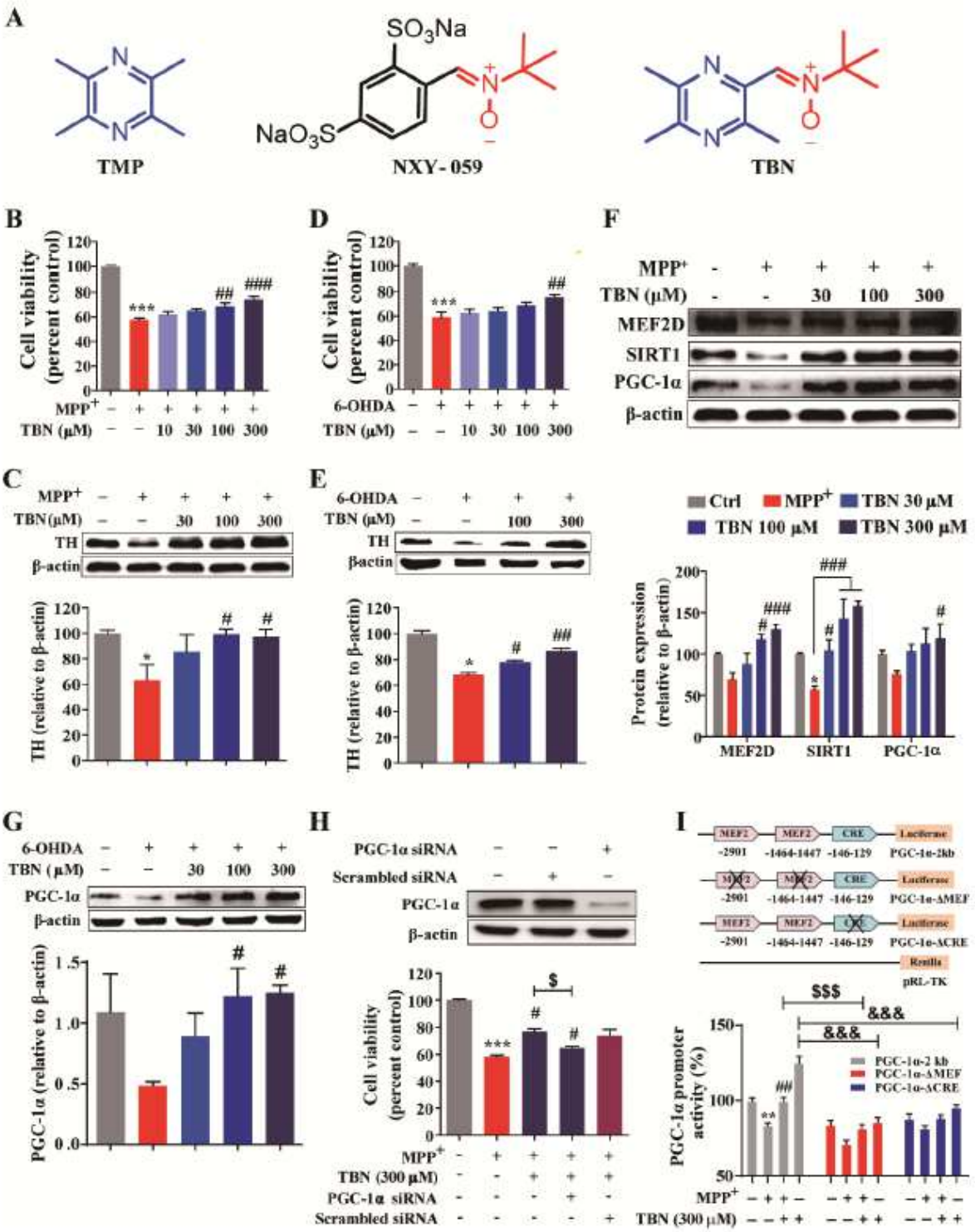

Figure 1

TBN protects primary midbrain neurons against MPP+ and 6-OHDA-induced toxicity through activation of PGC-1α. a Chemical structure of TMP, NXY-059 and TBN. Primary midbrain neurons were pre-treated with indicated concentrations of TBN for 2 h followed by treatment with 20 μM MPP+ or 30 μM 6-OHDA for 24

h (b-g). b, d Effect on cell viability of MPP+- or 6-OHDA-treated neurons. c, e Western blot for TH expression in MPP+- or 6- OHDA-treated neurons. f, g Western blot for expression of MEF2D, SIRT1 or PGC-1α in MPP+- or 6-OHDA-treated neurons. h Silencing of PGC-1α by specific siRNA abolished the protective effect of TBN in MPP+-treated neurons. i TBN increased MEF- and CRE- dependent PGC-1α promoter transcriptional activity. Data are expressed as means ± SEM of three independent experiments. *P < 0.05, **P < 0.01 and ***P < 0.001 versus untreated control group. #P < 0.05, ##P < 0.01 and ###P < 0.001 versus MPP+ or 6-OHDA alone group. $$$P < 0.001 and &&&P < 0.001. Data were analyzed using one-way ANOVA and Tukey's multiple comparison tests.

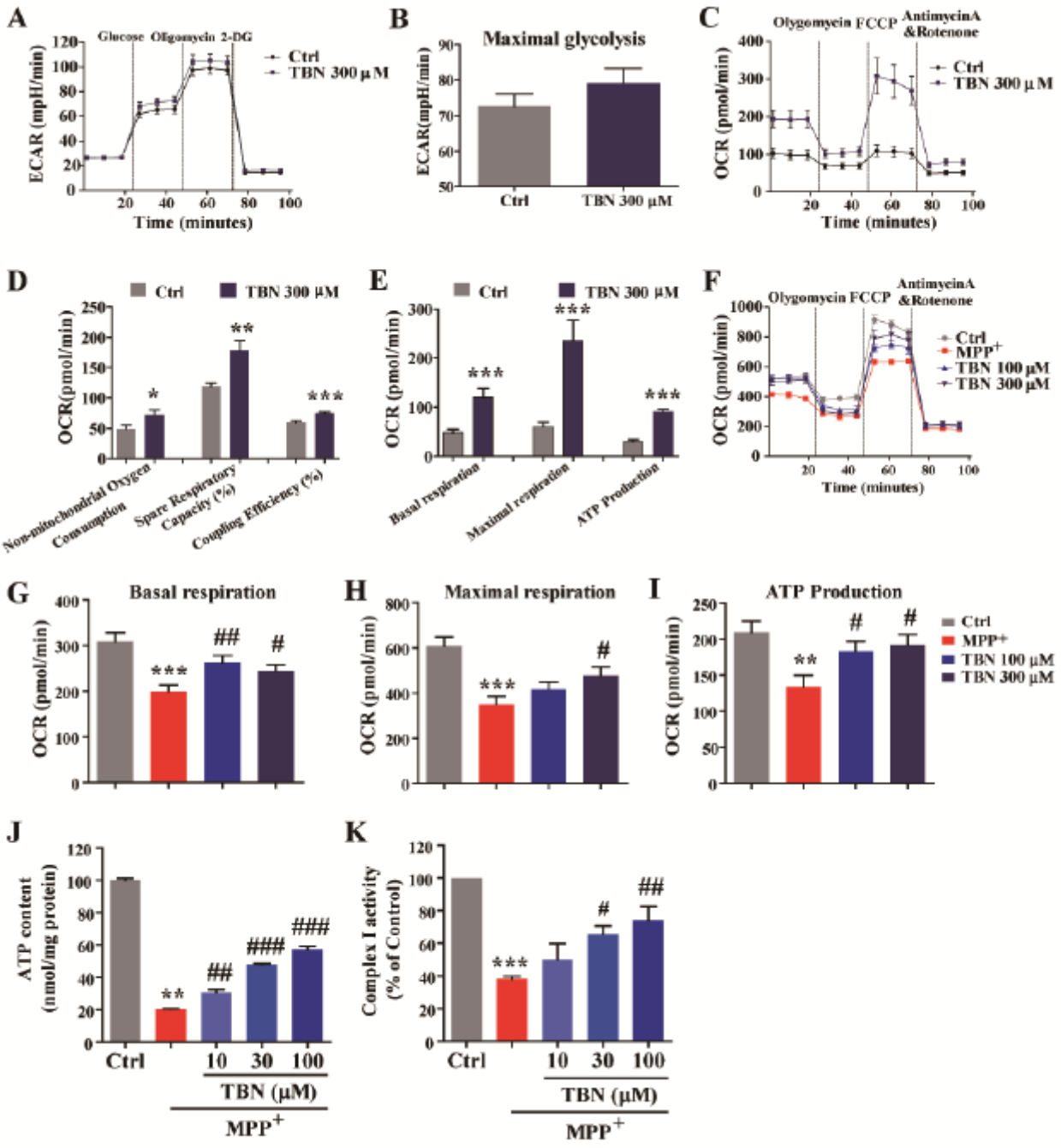

Figure 2

TBN increases PC12 cells mitochondrial functions. a, b ECAR response curve and maximal glycolysis. c-e OCR response curve and non-mitochondrial oxygen consumption, spared respiratory capacity (%), coupling efficiency (%), basal respiration, maximal respiration and ATP production. f Response curve of OCR after TBN treatment of MPP+- induced PC12 cells. g Basal respiration. h maximal respiration. i ATP production. j ATP content and (k) Mitochondrial complex I activity in CGNs. Data are means ± SEM of three independent experiments. *P < 0.05, **P < 0.01 and ***P < 0.001 versus untreated control group. #P < 0.05, ##P < 0.01 and ###P < 0.001 versus MPP+ alone group. Data were analyzed using unpaired Student's t test (b, d, e) or one-way ANOVA and Tukey's multiple comparison test (g-k).

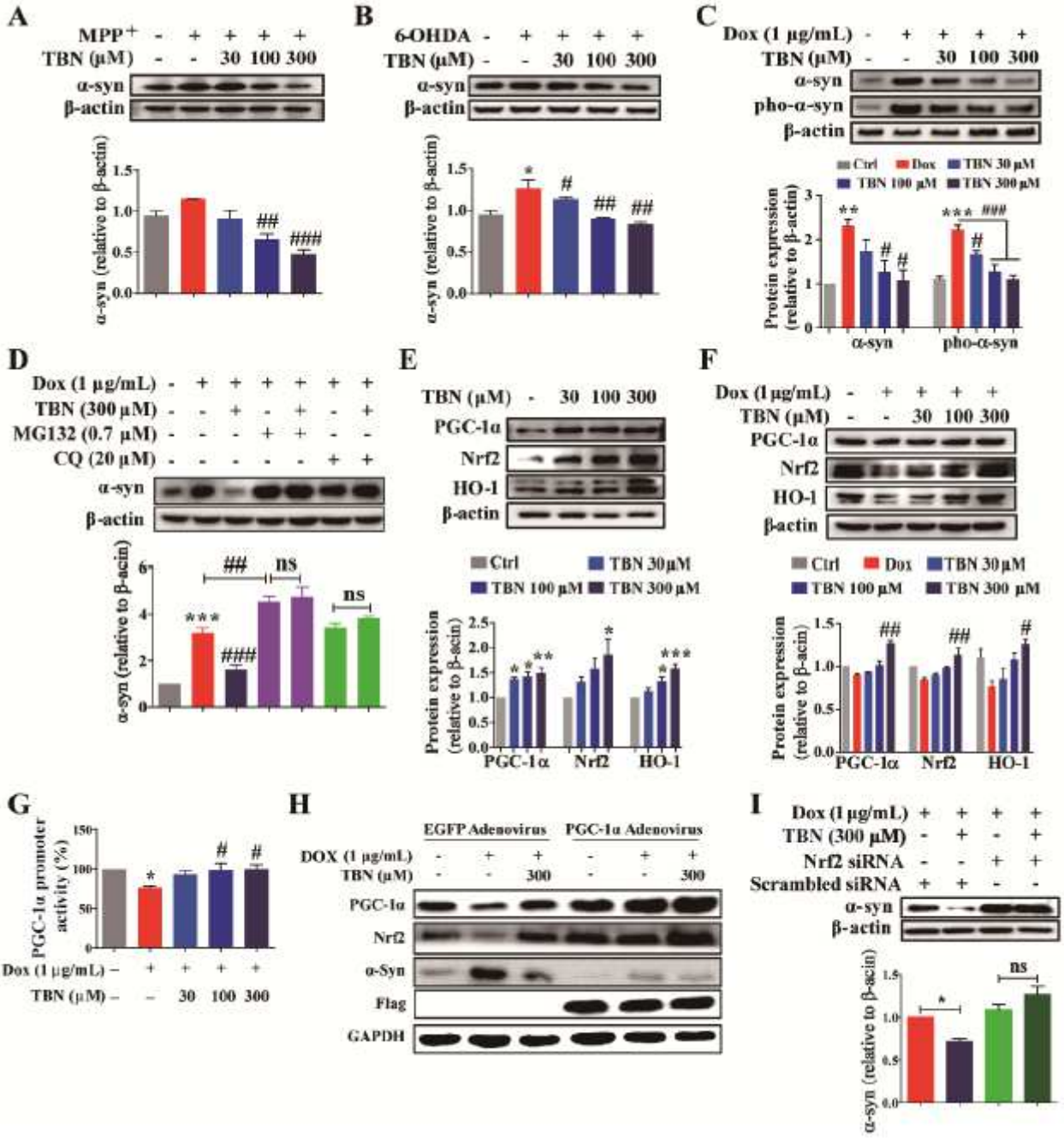

Figure 3

TBN promotes α-syn clearance through activation of PGC-1α/Nrf2. a, b Effect of TBN on the level of α-syn protein in SH-SY5Y cells with stable expression hA53T mutant α-syn, which were pre-treated with TBN at indicated concentrations for 2 h followed by 2 mM MPP+ (a) or 200 μM 6-OHDA (b) treatment for 24 h. c Effect of TBN on the protein levels of α-syn and pho-α-syn in PC12 cells with Dox-inducible expression of hA53T mutant α-syn, which were incubated with 1 μg/mL Dox in the presence or absence of TBN for another 24 h. d Both the proteasomal inhibitor MG132 and the lysosomal inhibitor CQ abolished the effect of TBN. Cells were pre-treated with 20 μM CQ or 0.7 μM MG132 for 2 h followed by treatment as in (c). e, f TBN concentration-dependently increased protein expression of PGC-1α, Nrf2 and HO-1 at basal (e) and Dox-stressed conditions (f) in PC12 cells with inducible expression of hA53T mutant α-syn. g TBN increased transcriptional activity of the PGC-1α promoter in Dox-induced PC12 cells. h Adenovirus-guided PGC-1α overexpression increased Nrf2 expression, but decreased α-syn levels in Dox-induced PC12 cells. i Down- regulation of Nrf2 by specific siRNA abolished the effect of TBN on α-syn clearance in Dox-induced PC12 cells. Data are means ± SEM of three independent experiments *P < 0.05, **P < 0.01 and ***P < 0.001 versus untreated control group. #P < 0.05, ##P < 0.01 and ###P < 0.001 versus MPP+ or 6-OHDA or Dox alone group. Data were analyzed using one-way ANOVA (a-i) and Tukey's multiple comparison tests.

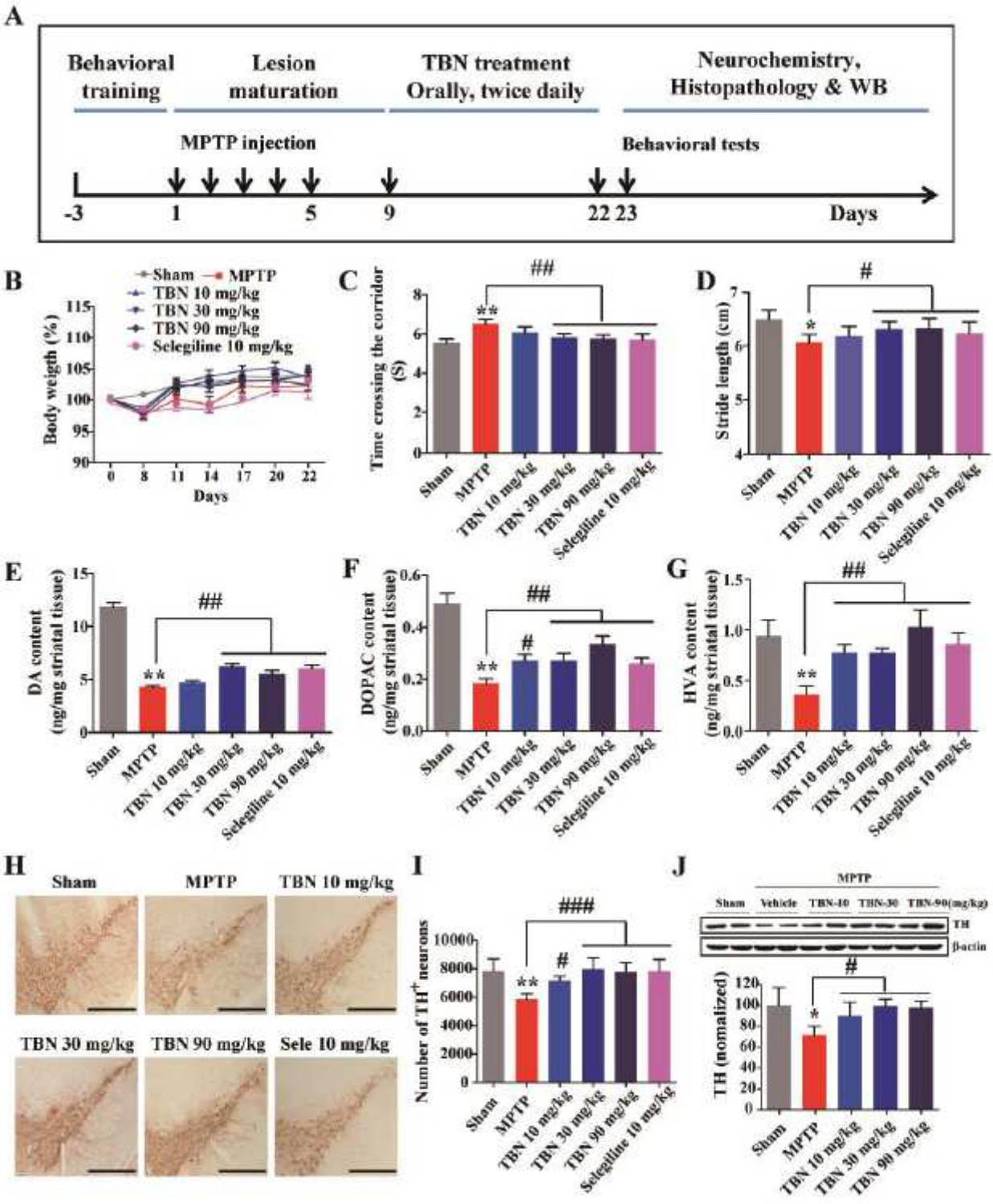

Figure 4

Fig. 4 TBN improves motor behavior and protects SN neurons in the MPTP-induced mice PD model. a Experimental schedule. b Body weight. c Time taken to cross the corridor (s). d Stride length (cm) in the footprint test. e-g Quantification of striatal DA, DOPAC and HVA by HPLC. h Representative photomicrographs of immunohistochemistry staining for TH in the SN of MPTP mice. Scale bars, 100 μm. i Stereological counting of TH-positive neurons from SN. j Western blot for TH expression in the SN

of MPTP mice. Data are means ± SEM of 15-16 mice per group in motor behavior test, and of 6-8 mice per group in biochemical, pathological and Western blot analyzes. *P < 0.05 and **P < 0.01 versus sham group; #P < 0.05, ##P < 0.01 and ###P < 0.001 versus MPTP alone group. Data were analyzed using one-way ANOVA and Tukey's multiple comparison tests.

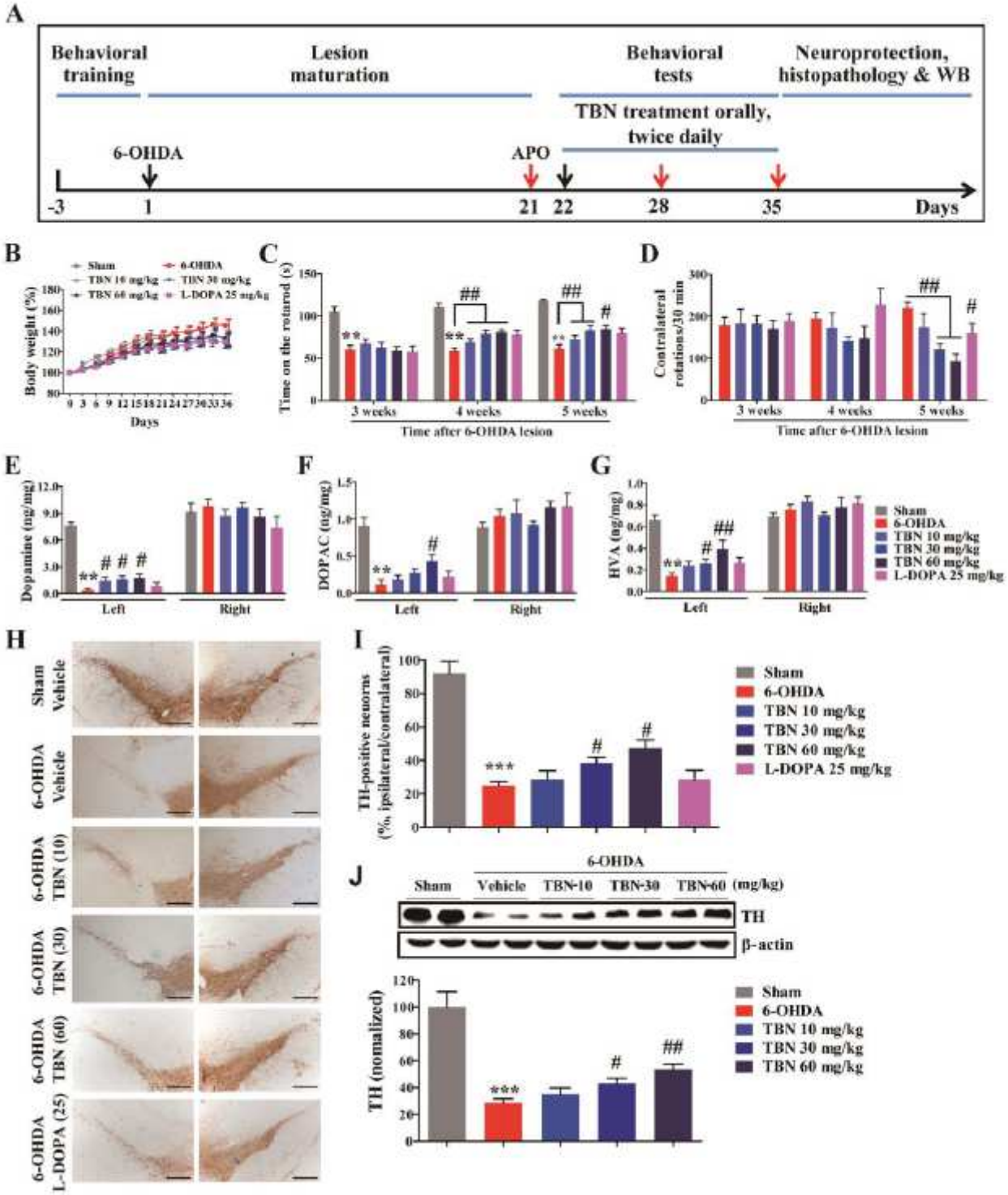

Figure 5

TBN improves motor behavior and protects SN neurons in the 6-OHDA-induced rat PD model. a Experimental schedule. b Body weight. c Time on the rotarod (s). d Contralateral rotations in 30 min after APO injection. e-g Quantification of striatal DA, DOPAC and HVA by HPLC. h Representative photomicrographs of immunohistochemistry staining for TH in SN. Scale bars, 200 μm. i Stereological counting of TH-positive neurons from SN. j Western blot for TH expression in SN of 6-OHDA rats. Data were means ± SEM of 9-13 rats per group in motor behavior test, and of 5-7 rats per group in biochemical, pathological and Western blot analyses. **P < 0.01 and ***P < 0.001 versus sham group; #P < 0.05 and ##P < 0.01 versus 6-OHDA alone group. Data were analyzed using two-way (b-d) or one-way ANOVA (e-j) and Tukey's multiple comparison tests.

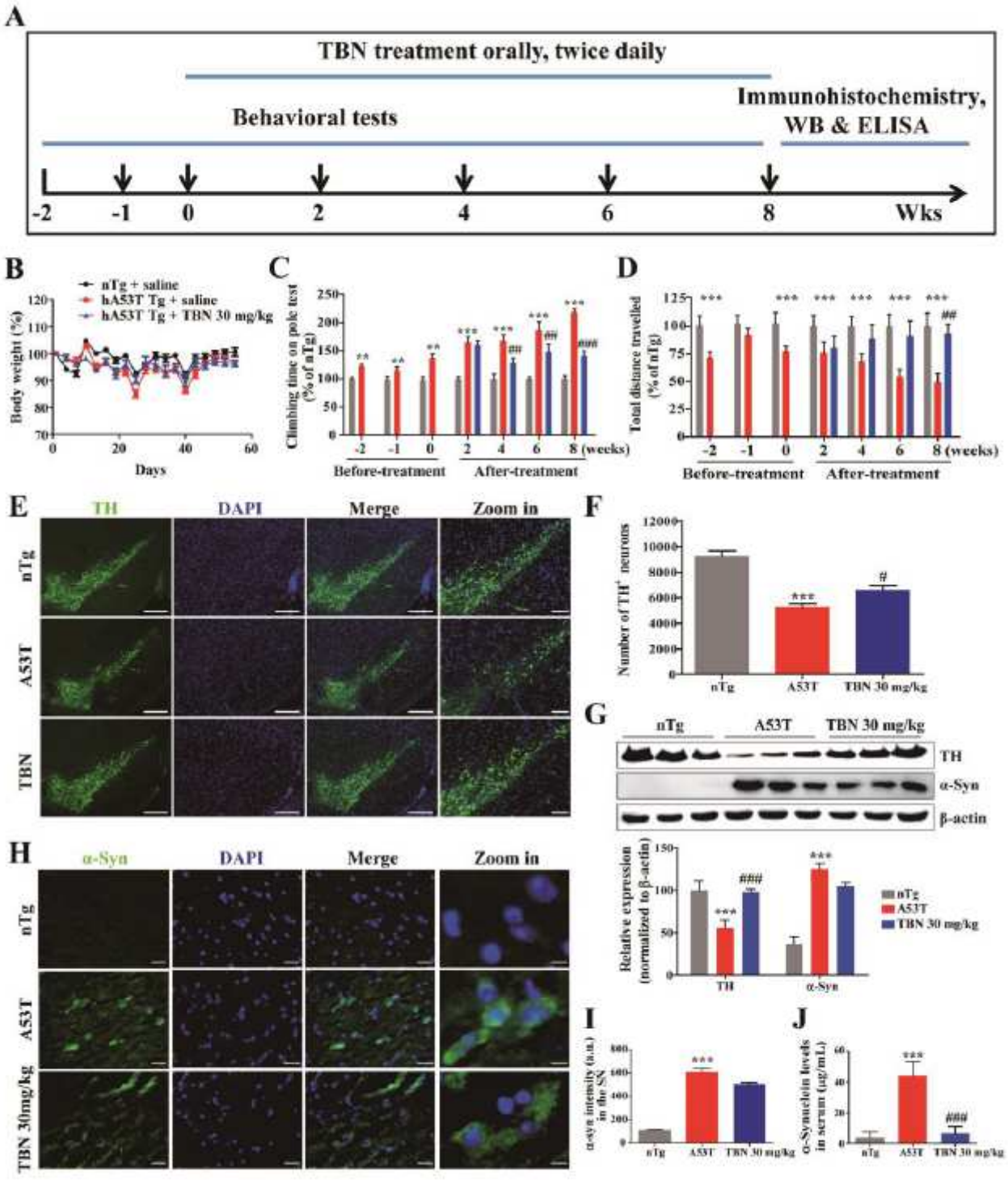

Figure 6

TBN improves motor behavior and protects SN neurons in the hA53T α-syn transgenic mice PD model. a Experimental schedule. b Body weight. c Climbing time on pole test (% of nTg). d Total distance travelled (% of nTg). e Representative photomicrographs of immunofluorescence staining for TH in SN. Scale bars, 100 μm, but 50 μm for zoon in. f Stereological counting of TH-positive neurons from SN. g Western blot for TH and α-syn expression in SN of hA53T α-syn transgenic mice. h Representative photomicrographs

of immunofluorescence staining for α-syn in brain sections. Scale bars, 50 μm, but 10 μm when zoomed in. i Intensity of α-syn in the SN [a.u. (arbitrary units)]. j Quantification of α-syn contents in the serum by ELISA. Data are means ± SEM of 7-9 mice per group for all measurements. **P < 0.01 and ***P < 0.001 versus nTg group; #P < 0.05, ##P < 0.01 and ###P< 0.001 versus hA53T α-syn Tg mice model group. Data were analyzed using two-way (b-d) or one-way ANOVA (f, g, i and j) and Tukey's multiple comparison tests.

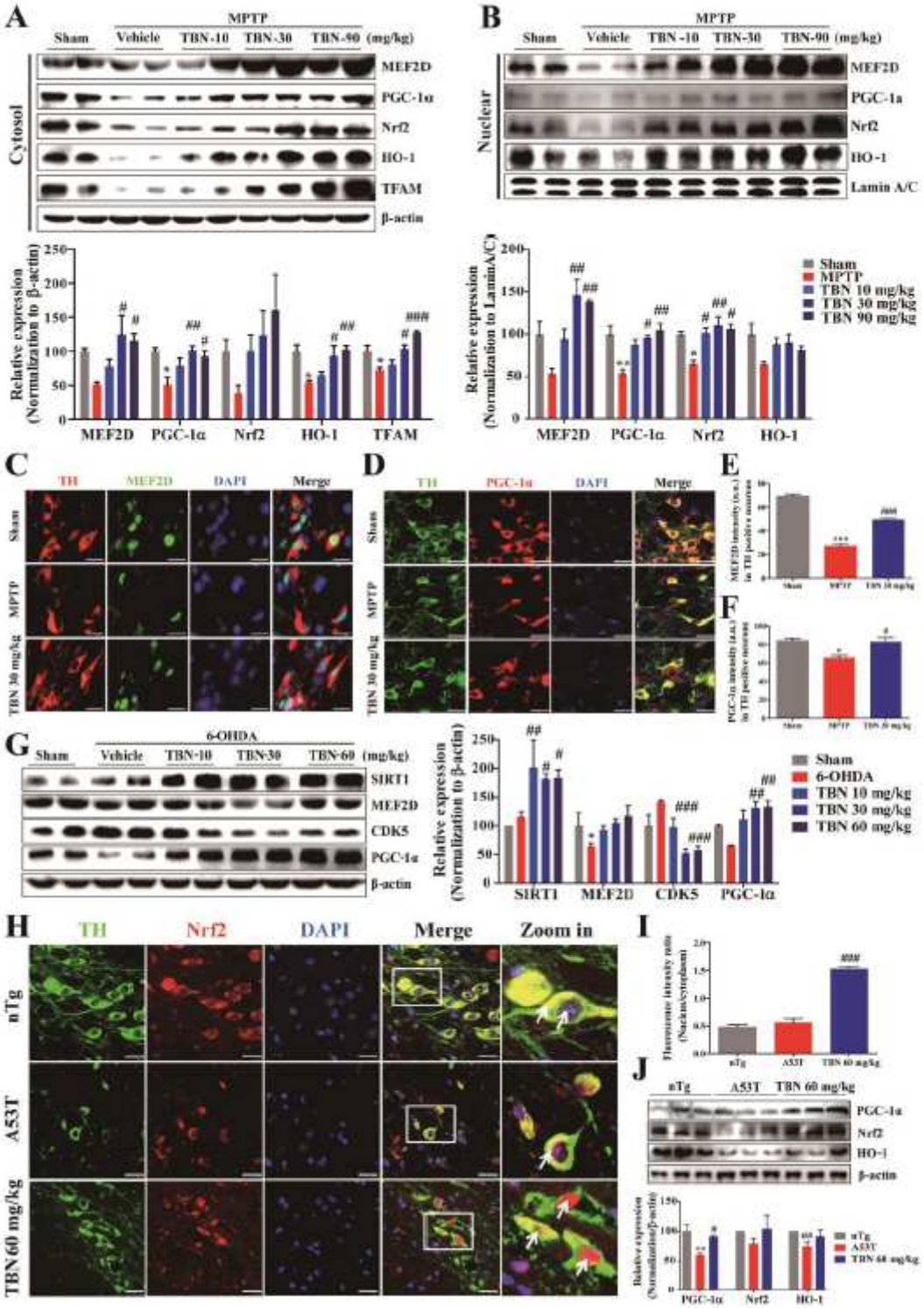

Figure 7

TBN activates PGC-1α/Nrf2 pathway in the animal PD models. a Western blot for expression of MEF2D, PGC-1α, Nrf2, HO-1 and TFAM in the cytosol of SN tissue from MPTP mice. b Western blot for expression of MEF2D, PGC-1α, Nrf2, and HO-1 in the nuclei of SN tissue from MPTP mice. c, d Representative photomicrographs of co- immunofluorescence staining for TH (red), MEF2D (green), and DAPI (blue) (c), and for TH (green), PGC-1α (red), and DAPI (blue) (d) in the SN of MPTP mice. Scale bars, 20 μm. e, f Intensity of MEF2D and PGC-1α in the TH-positive neurons. g Western blot for expression of SIRT1, MEF2D, CDK5 and PGC-1α in the SN of 6-OHDA rats. h Representative photomicrographs of co-immunofluorescence for TH (green), Nrf2 (red), and DAPI (blue) in the SN of hA53T Tg mice. Scale bars, 25 μm. Boxed areas are shown at a higher magnification in the right panel. Arrows indicate co-localization of TH and Nrf2, and nuclear translocation of Nrf2. i Fluorescence intensity ratio of Nrf2 in the TH-positive neurons. j Western blot for expression of PGC-1α, HO-1, and Nrf2 in the SN of hA53T Tg mice. Data were means ± SEM of 6 animals per group. *P < 0.05, **P < 0.01 and ***P < 0.001 versus sham or nTg group; #P < 0.05, ##P < 0.01 and ###P < 0.001 versus model group. Data were analyzed using one-way ANOVA and Tukey's multiple comparison tests.

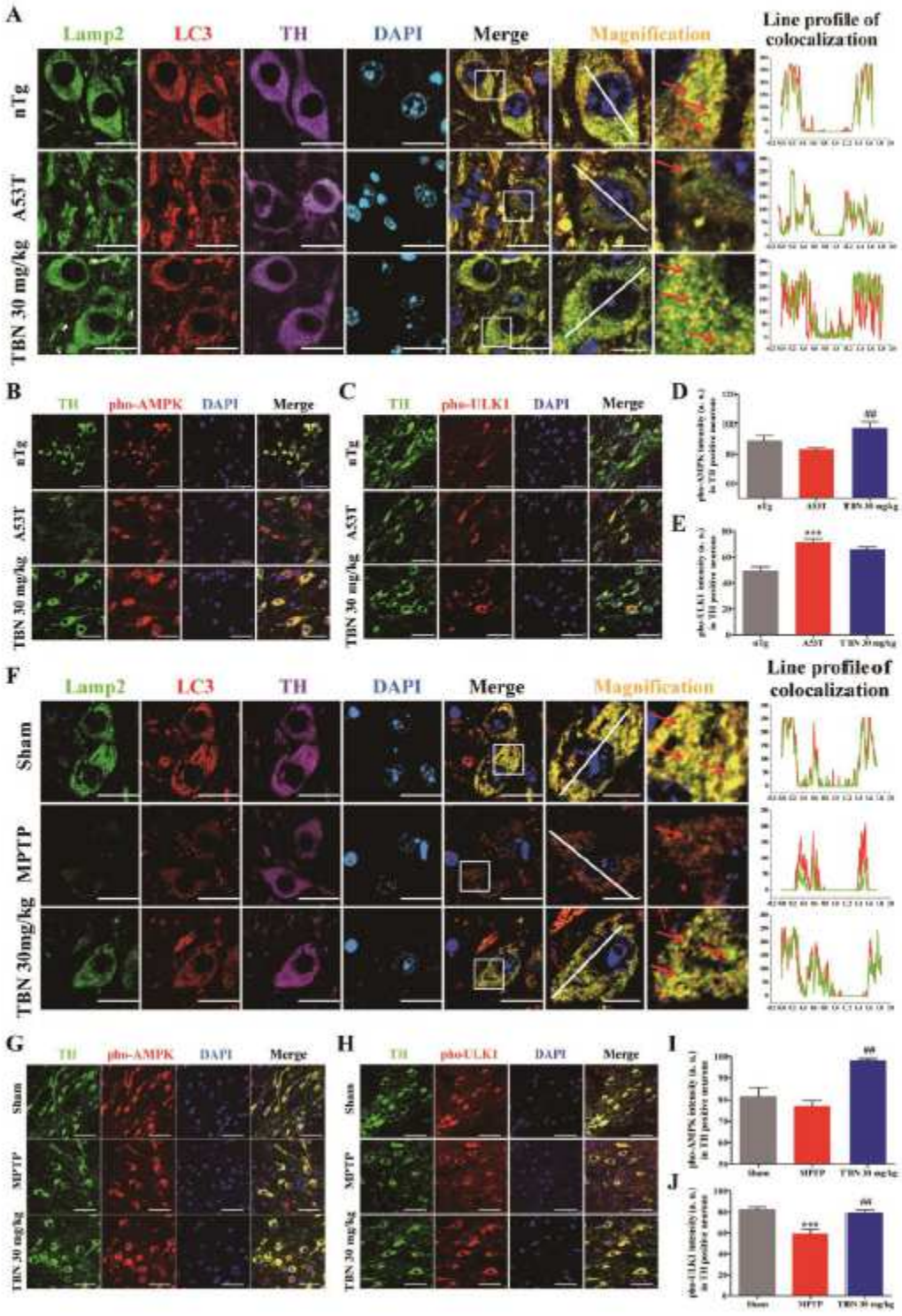

Figure 8

Fig. 8 TBN activates autophagy in hA53T α-syn Tg and MPTP-induced mice PD model. a-c Representative photomicrographs of co-immunofluorescence staining for Lamp2 (green), LC3 (red), TH (purple) and DAPI (light blue) (a), for TH (green), pho-AMPK (Thr 172) (red) and DAPI (blue) (b), and for TH (green), pho-ULK1 (Ser 757) (red) and DAPI (blue) (c) in the SN of hA53T α-syn Tg mice. Scale bars, 20 μm, but 10 μm when zoomed in. d, e Intensity of pho-AMPK (Thr 172) and pho-ULK1 (Ser 757) in the TH-positive

neurons [a.u.(arbitrary units)]. f-h Representative photomicrographs of co-immunofluorescence staining for Lamp2 (green), LC3 (red), TH (purple) and DAPI (light blue) (f), for TH (green), pho-AMPK (Thr 172) (red) and DAPI (blue) (g), and for TH (green), pho-ULK1 (Ser 555) (red) and DAPI (blue) (h) in the SN of MPTP mice. Scale bars, 20 μm, but 10 μm when zoomed in. i, j Intensity of pho-AMPK (Thr 172) and pho-ULK1 (Ser 555) in the TH-positive neurons [a.u. (arbitrary units)]. Boxed areas in a and f are shown at a higher magnification in the right panel. Arrows indicate co-localization of Lamp2, LC3 and TH. The co-localization between LC3 and Lamp2 are illustrated by line profile. ***P < 0.001 versus sham or nTg group; ##P < 0.01 versus model group. Data were analyzed using one-way ANOVA and Tukey's multiple comparison tests.

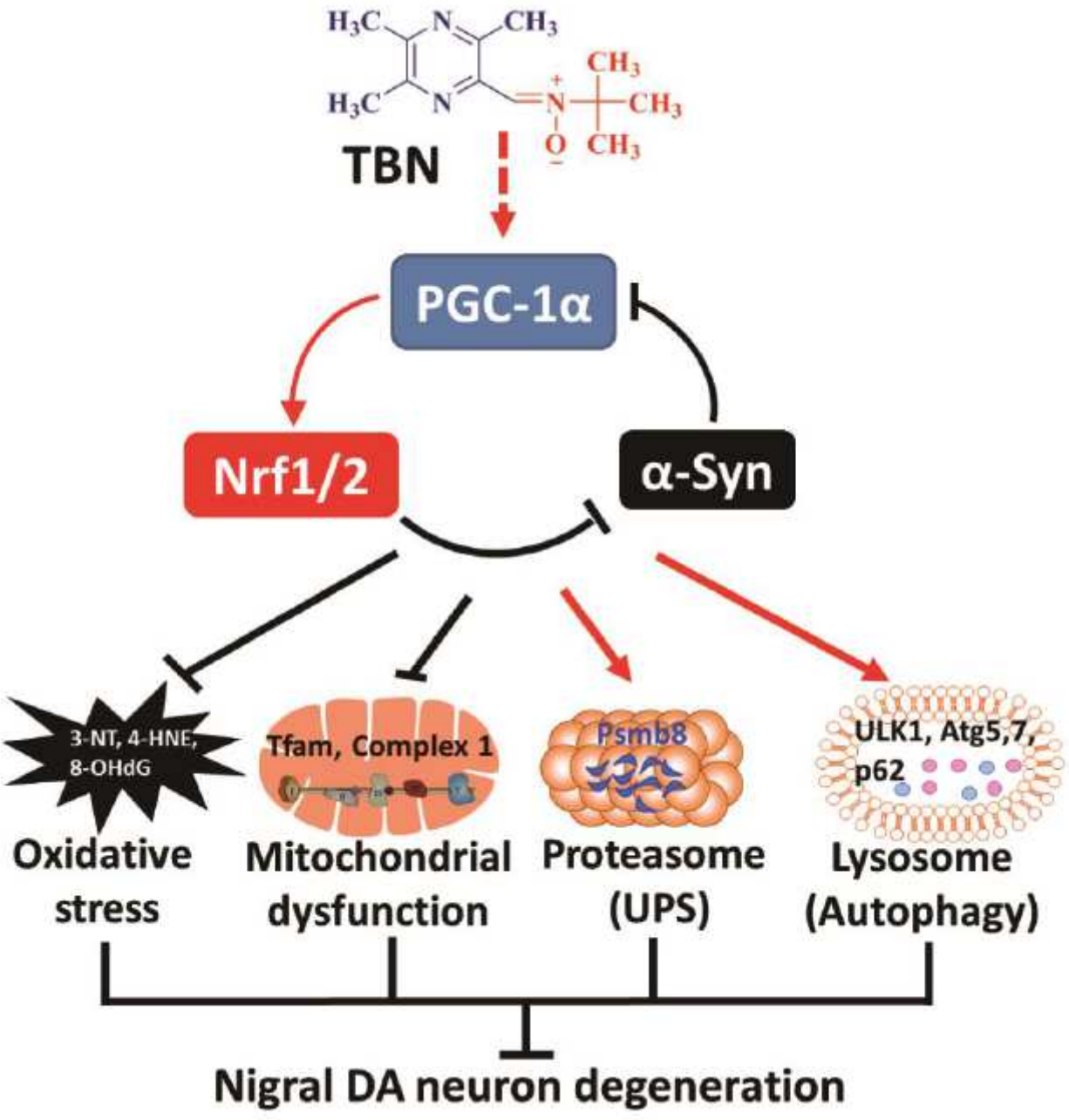

Figure 9

Schematic diagram of proposed TBN's mechanisms of action in experimental PD models. TBN suppresses oxidative stress to activate the AMPK/PGC-1α/Nrf1/2 signaling pathway, resulting in reduced oxidative stress, enhanced mitochondrial function and increased protein clearance, eventually preventing the advance of nigral dopaminergic neurodegeneration in experimental models of PD.

Supplementary Files

This is a list of supplementary files associated with this preprint. Click to download.

- Additionaldocumentation.doc